

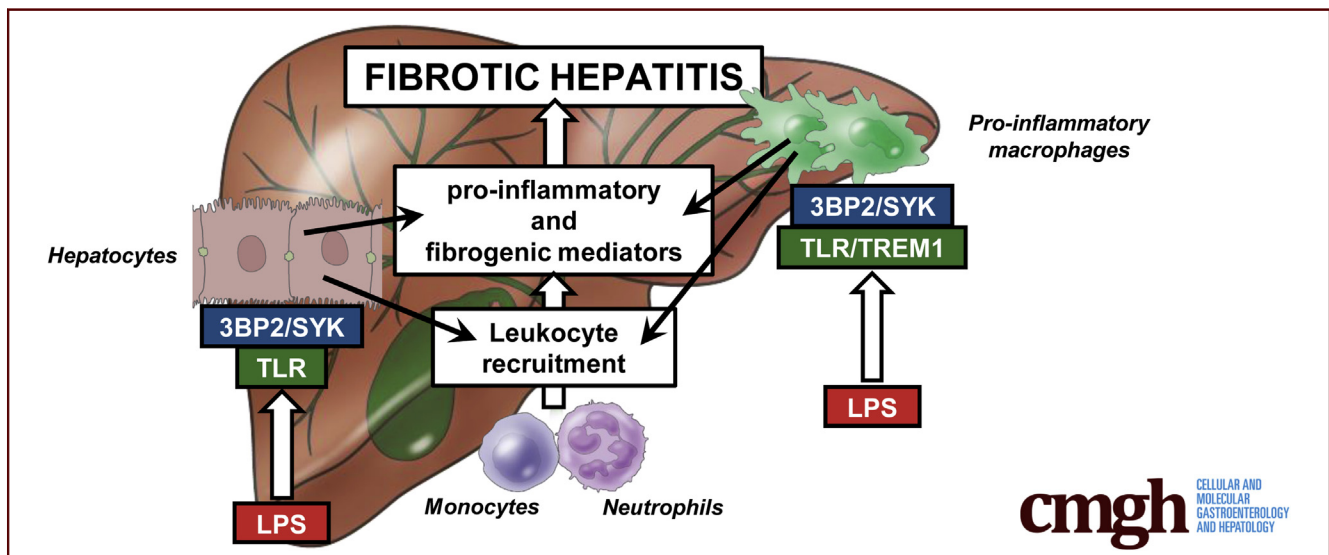
## ORIGINAL RESEARCH

## SYK-3BP2 Pathway Activity in Parenchymal and Myeloid Cells Is a Key Pathogenic Factor in Metabolic Steatohepatitis



Carmelo Luci,<sup>1,a</sup> Elodie Vieira,<sup>1,a</sup> Manon Bourinet,<sup>1</sup> Déborah Rousseau,<sup>1</sup> Stéphanie Bonnafous,<sup>2</sup> Stéphanie Patouraux,<sup>2</sup> Lauren Lefevre,<sup>1</sup> Frederic Larbret,<sup>1</sup> Virginie Prod'homme,<sup>1</sup> Antonio Iannelli,<sup>2</sup> Albert Tran,<sup>2</sup> Rodolphe Anty,<sup>2</sup> Béatrice Bailly-Maitre,<sup>1</sup> Marcel Deckert,<sup>1,b</sup> and Philippe Gual<sup>1,b</sup>

<sup>1</sup>Université Côte d'Azur, INSERM, U1065, C3M, Nice, France; and <sup>2</sup>Université Côte d'Azur, CHU, INSERM, U1065, C3M, Nice, France



## SUMMARY

This work reports that SYK-3BP2 pathway activity enhances the LPS-TLR4 responses in both hepatocytes and resident liver macrophages. This initiates the onset of local inflammation and contributes to liver accumulation of leukocytes. Targeting of 3BP2 or SYK prevents metabolic steatohepatitis features.

**BACKGROUND & AIMS:** Spleen tyrosine kinase (SYK) signaling pathway regulates critical processes in innate immunity, but its role in parenchymal cells remains elusive in chronic liver diseases. We investigate the relative contribution of SYK and its substrate c-Abl Src homology 3 domain-binding protein-2 (3BP2) in both myeloid cells and hepatocytes in the onset of metabolic steatohepatitis.

**METHODS:** Hepatic SYK-3BP2 pathway was evaluated in mouse models of metabolic-associated fatty liver diseases (MAFLD) and in obese patients with biopsy-proven MAFLD (n = 33). Its role in liver complications was evaluated in *Sh3bp2* KO and myeloid-specific *Syk* KO mice challenged with

methionine and choline deficient diet and in homozygous *Sh3bp2*<sup>KI/KI</sup> mice with and without SYK expression in myeloid cells.

**RESULTS:** Here we report that hepatic expression of 3BP2 and SYK correlated with metabolic steatohepatitis severity in mice. 3BP2 deficiency and SYK deletion in myeloid cells mediated the same protective effects on liver inflammation, injury, and fibrosis priming upon diet-induced steatohepatitis. In primary hepatocytes, the targeting of 3BP2 or SYK strongly decreased the lipopolysaccharide-mediated inflammatory mediator expression and 3BP2-regulated SYK expression. In homozygous *Sh3bp2*<sup>KI/KI</sup> mice, the chronic inflammation mediated by the proteasome-resistant 3BP2 mutant promoted severe hepatitis and liver fibrosis with augmented liver SYK expression. In these mice, the deletion of SYK in myeloid cells was sufficient to prevent these liver lesions. The hepatic expression of SYK is also up-regulated with metabolic steatohepatitis and correlates with liver macrophages in biopsy-proven MAFLD patients.

**CONCLUSIONS:** Collectively, these data suggest an important role for the SYK-3BP2 pathway in the pathogenesis of chronic liver inflammatory diseases and highlight its targeting in hepatocytes and myeloid cells as a potential strategy to treat

metabolic steatohepatitis. (*Cell Mol Gastroenterol Hepatol* 2022;13:173–191; <https://doi.org/10.1016/j.jcmgh.2021.08.004>)

**Keywords:** SYK; 3BP2; TREM1; TLR4; MAFLD; NASH; Fibrosis.

**M**etabolic-associated fatty liver diseases (MAFLD)<sup>1</sup> are the most common chronic liver diseases worldwide, with a global prevalence of 25%.<sup>2</sup> The burden of MAFLD is increasing in parallel with the global obesity epidemic<sup>3</sup> and still presents an unmet medical need with no approved pharmacologic therapies. MAFLD is a broad term that encompasses the full spectrum of fatty liver diseases from simple hepatic steatosis to metabolic steatohepatitis, fibrosis/cirrhosis, and hepatocellular cancer. Obesity and metabolic syndrome are also associated with the development of MAFLD. Similarly, type 2 diabetes mellitus, insulin resistance, hypertension, and weight gain are risk factors for MAFLD progression.<sup>4,5</sup> However, the inverse relationship also exists, with MAFLD being a risk factor for many metabolic diseases including type 2 diabetes<sup>6</sup> and cardiovascular diseases.<sup>7</sup>


In addition to genetic and environmental factors, the interaction of gut and adipose tissue with the liver enhances liver metabolic disorders (steatosis and insulin resistance), chronic inflammation, and injury-mediated fibrosis.<sup>8,9</sup> In MAFLD liver, a large number of innate immune cells are involved in the onset of the chronic inflammation, including resident and recruited macrophages and neutrophils but also parenchymal hepatocytes.<sup>8,9</sup> Stressed hepatocytes, such as fatty and sub-lethal hepatocytes, take on an immune function by sensing excessive metabolite levels and pathogen- and damage-associated molecular patterns (PAMPs and DAMPs, respectively), which in turn elicit inflammatory events associated with metabolic dysfunction.<sup>10</sup> Macrophages also play a central role in the development and progression of MAFLD.<sup>11,12</sup> Liver-resident macrophages (Kupffer cells) can initiate inflammation and help to recruit blood-derived monocytes. The polarization of both resident and recruited macrophages into pro-inflammatory phenotypes subsequently promotes MAFLD progression. The gut-derived endotoxins, lipids, and molecules associated with hepatocellular damage and death (DAMPs, extracellular vesicles, apoptotic bodies, etc) are the main factors contributing to macrophage and hepatic stellate cell (HSC) activation and the regulation of chronic hepatitis and fibrogenesis. To study pathways that are conserved in both hepatocytes and macrophages and involved in the steatosis-steatohepatitis transition, we focused on the role of the spleen tyrosine kinase (SYK) pathway in the regulation of inflammatory mediators.

SYK is a cytoplasmic non-receptor tyrosine kinase, and SYK-dependent signaling is known to regulate critical processes in innate and adaptive immunity downstream immunoreceptors (including B-cell receptors, T-cell receptors, and Fc receptors), C-type lectins receptors, integrins, and toll-like receptors (TLRs).<sup>13–16</sup> In the liver, SYK is highly expressed in HSCs and inflammatory cells including macrophages.<sup>17,18</sup> SYK is also overexpressed in balloon

hepatocytes containing Mallory-Denk bodies,<sup>19</sup> a hallmark of chronic liver diseases such as MAFLD and alcoholic liver diseases. Recent studies have reported a pathogenic role for SYK in liver fibrosis,<sup>17,18</sup> as previously reported in certain fibrotic-related diseases including scleroderma, renal fibrosis, and rheumatoid arthritis.<sup>20–22</sup> SYK inhibitors blocked HSC activation *in vitro* and in animal models of hepatic fibrosis, including toxin challenge (carbon tetrachloride, thioacetamide [TAA], N-nitrosodiethylamine)- and bile duct ligation-induced liver fibrosis models.<sup>17</sup> In addition, SYK inhibitors potently attenuated liver fibrosis and hepatocellular carcinoma development in N-nitrosodiethylamine and N-nitrosodiethylamine/carbon tetrachloride animal models.<sup>17,18</sup> Interestingly, SYK deletion in the myeloid compartment conferred protection against fibrogenic progression upon TAA-mediated liver injury.<sup>18</sup> The regulation of macrophage activity by SYK in the context of liver injury and exacerbated by DAMPs could provide an attractive mechanism in chronic liver diseases. This exacerbated activation of macrophages by TLR ligands (DAMPs, PAMPs, and saturated lipids) was found to be a central pathogenic mechanism for chronic inflammation and MAFLD. In addition, TREM1, a member of the triggering receptors expressed on myeloid cells (TREM) family that mediates the inflammatory response through TLR4, DNAX-activation protein of 12 kDa (DAP12), and SYK, has been implicated in liver diseases.<sup>23–25</sup> In line with the important role of the SYK pathway in inflammatory diseases, gain-of-function mutations in SYK, leading to increased phosphorylation and hyperactivated downstream signaling, were recently associated with immune dysfunction and systemic inflammation.<sup>26</sup> Among the components of the SYK pathway,<sup>13</sup> we have previously shown that 3BP2 (also known as SH3 binding protein 2), a cytoplasmic adapter that interacts with SYK,<sup>27–30</sup> was necessary for TLR-mediated activation of macrophages in response to PAMPs and DAMPs. Indeed, 3BP2-deficient macrophages exhibited dramatically reduced inflammatory responses to microbial challenge and reduced phagocytosis.<sup>31</sup> Remarkably, mutations in *SH3BP2* that were found in the human genetic disease cherubism<sup>32</sup> have been associated in mice with systemic autoinflammation, SYK hyperphosphorylation, and elevated TLR signaling in

<sup>a</sup>Authors share co-first authorship; <sup>b</sup>Authors share co-senior authorship.

**Abbreviations used in this paper:** ALT, alanine aminotransferase; AST, aspartate aminotransferase; 3BP2, c-Abl Src homology 3 domain-binding protein-2; DAMP, damage-associated molecular pattern; HFD, high-fat diet; HSC, hepatic stellate cell; LPS, lipopolysaccharide; MAFLD, metabolic-associated fatty liver diseases; MCDD, methionine and choline deficient diet; PAMP, pathogen-associated molecular pattern; PCR, polymerase chain reaction; PPAR $\alpha$ , peroxisome proliferator activated receptor alpha; SD, standard deviation; SYK, spleen tyrosine kinase; TAA, thioacetamide; TLR4, toll-like receptor 4; TNF, tumor necrosis factor; TREM, triggering receptors expressed on myeloid cells; Wt, wild-type.

 Most current article

© 2021 The Authors. Published by Elsevier Inc. on behalf of the AGA Institute. This is an open access article under the CC BY-NC-ND license (<http://creativecommons.org/licenses/by-nc-nd/4.0/>).

2352-345X

<https://doi.org/10.1016/j.jcmgh.2021.08.004>

myeloid cells carrying homozygous *Sh3bp2* cherubic mutations (*Sh3bp2*<sup>K1/K1</sup> animals).<sup>31,33–35</sup> Furthermore, we found that a hemizygous *Sh3bp2* cherubic mutation enhanced macrophage responsiveness to TLR ligands.<sup>31</sup> Importantly, both deletion of SYK in myeloid cells<sup>36</sup> and targeting the SYK/3BP2 axis<sup>37</sup> ameliorated the chronic inflammation driven by the mutation of 3BP2 in mice.

Although SYK and its signaling partner 3BP2 are expressed in liver tissue, many details are still elusive, such as their relative local expression in response to liver status and their relative pathogenic roles in hepatocytes and macrophages throughout the development of liver steatosis and progression to steatohepatitis. We thus investigated these open questions in different mouse models of MAFLD, human MAFLD samples, and transgenic animals deficient in 3BP2 or SYK signaling or with sustained activation of 3BP2 signaling (cherubic 3BP2 mutants).

## Results

### Hepatic Expression of 3BP2 and SYK Correlated With Liver Complications in Mouse Models of MAFLD

We first evaluated the hepatic expression levels of *Sh3bp2*, *Syk*, and macrophage marker *Emr1* (F4/80) in a dietary mouse model of obesity and hepatic steatosis. After 33 weeks of high-fat diet (HFD), the wild-type C57BL/6 (Wt) mice developed obesity, hepatic injury as evaluated by alanine aminotransferase (ALT) activity, and severe hepatic steatosis (Figure 1A–C). The hepatic expression levels of *Syk* and *Emr1* were increased upon 33 weeks of HFD (Figure 1D) and hepatic expression of *Syk* correlated with hepatic steatosis, ALT activity, and hepatic expression of *Emr1* (Figure 1E). The hepatic expression levels of *Sh3bp2* tended to increase with liver complications (Figure 1D). To subsequently investigate the behavior of the 3BP2 and SYK in response to the progression and the severity of the MAFLD, we monitored hepatic expression in Wt mice fed a diet deficient in methionine and choline (MCDD) for 2 and 7 weeks. The duration of the MCDD challenge correlates with the severity of the steatohepatitis associated with the aggravation of liver injury and fibrogenesis. At 2 weeks, mice developed moderate hepatic steatosis with mild hepatic inflammation (as evaluated by the inflammatory foci number) and liver injury (Figure 2A–C). The long-lasting MCDD challenge (7 weeks) aggravated the liver complications with severe steatosis, inflammation, and liver injury (Figure 2A–C). Hepatic *Sh3bp2* and *Syk* expression levels were progressively increased with the MAFLD severity (Figure 2D). Hepatic *Sh3bp2* and *Syk* also strongly correlated with hepatic steatosis, inflammatory foci number, liver injury, and hepatic expression of *Emr1* (Figure 2E). Upon 7 weeks of MCDD challenge, the increased *Syk* expression was due to the up-regulation of both isoforms of *Syk* (*Syk-b* (S) and *Syk* (L)) (the latter being the main isoform expressed in liver) (Figure 2F). The hepatic expression levels of SYK were also increased upon MCDD at the protein level (Figure 2G). We then evaluated which cell types in the liver were responsible for 3BP2 and SYK expression. *Sh3bp2* and

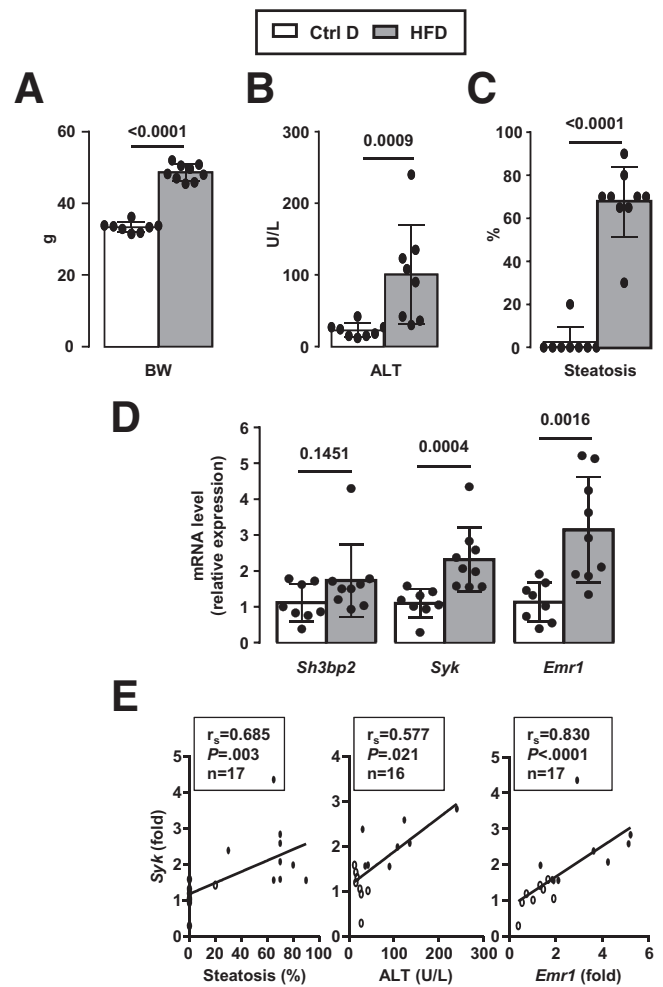
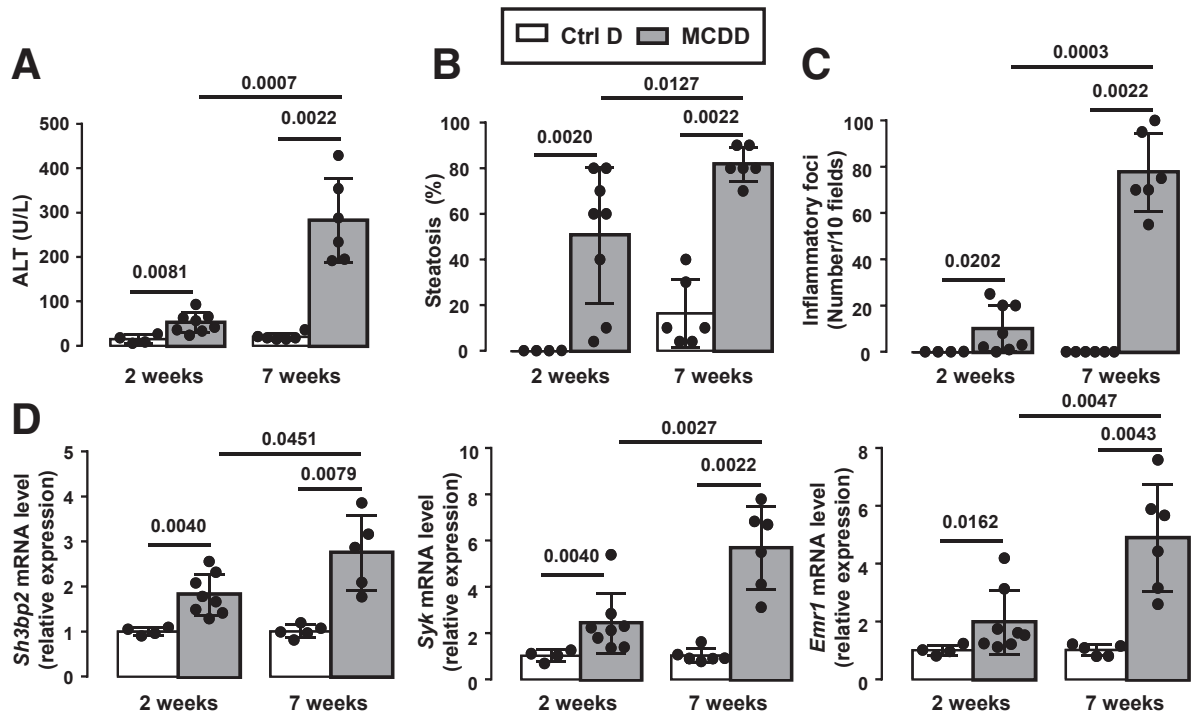


**Figure 1. Hepatic expression of SYK correlated with hepatic steatosis, liver injury, and macrophage marker expression in HFD-fed mice.** Wild-type mice fed a control diet (Ctrl D) or HFD for 33 weeks (8–9 mice/group). Body weight (BW) (A), serum ALT activity (B), and hepatic steatosis (on H&E stained liver tissue section) (C) have been evaluated. (D) Hepatic expression of *Sh3bp2*, *Syk*, and *Emr1* was evaluated in mice as indicated by mRNA level. Gene expression values were normalized to mRNA levels of *36b4*. Results are expressed relative to expression level in controls. (E) Correlation between hepatic expression of *Syk* with hepatic steatosis (%), ALT activity, and hepatic *Emr1* expression were analyzed using the Spearman's correlation test. (A–D) Results are expressed as means  $\pm$  standard deviation (SD) and statistically analyzed using the Mann-Whitney test.

*Syk* expression at the mRNA level was detected in hepatocytes and non-parenchymal fraction from non-pathogenic liver in lean mice (Figure 2H). *Sh3bp2* was expressed at higher levels than *Syk* in hepatocytes. In addition, *Sh3bp2* and *Syk* were highly expressed in non-parenchymal cells compared with *Syk* expression in hepatocytes with higher expression of *Syk* than *Sh3bp2*. Therefore, these results indicate that 3BP2 and SYK could impact the functions of both hepatocytes and non-parenchymal cells. In addition, the up-regulation of 3BP2 and SYK with MAFLD severity suggests a potential role in the steatosis-steatohepatitis transition.

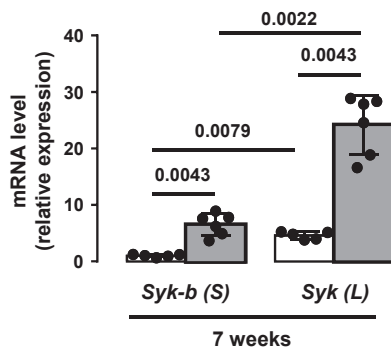


**E**

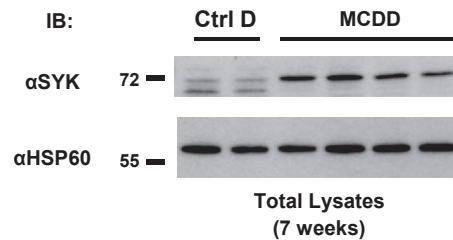
	Steatosis (%)			ALT (U/L)			Inflammatory foci (Nb/10 fields)			Liver <i>Emr1</i> (fold)		
	r	P	N	r	P	N	r	P	N	r	P	N
Liver <i>Sh3bp2</i> (fold)	0.900	<0.0001	22	0.802	<0.0001	22	0.826	0.0001	22	0.870	<0.0001	22
Liver <i>Syk</i> (fold)	0.876	<0.0001	24	0.802	<0.0001	24	0.901	<0.0001	24	0.938	<0.0001	24

Spearman's rank correlation test.

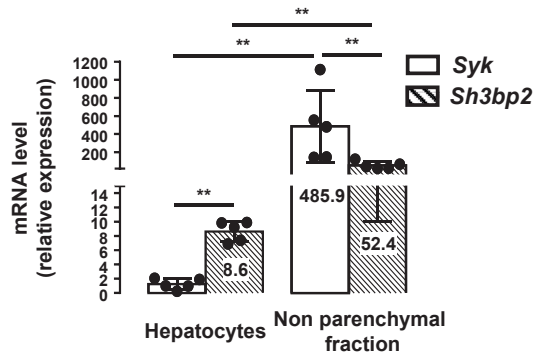
**F**



**G**



**H**



### 3BP2 Deficiency Partially Prevented Liver Injury, Hepatic Steatosis, and Steatohepatitis Induced by MCDD Challenge

The role of 3BP2 in liver injury and steatohepatitis induced by MCDD was then investigated using mice deficient for 3BP2. The MCDD challenge was associated with elevated hepatic *Sh3bp2* expression in Wt mice (Figure 3A). The *Sh3bp2*<sup>-/-</sup> mice displayed less liver damage as shown by the lower ALT activity levels (Figure 3B). Furthermore, histologic analyses demonstrated less hepatic steatosis and inflammatory foci in the livers of MCDD-fed *Sh3bp2*<sup>-/-</sup> mice compared with livers of MCDD-fed Wt mice (Figure 3C and D). The decreased inflammatory foci number was associated with partial prevention of the recruitment of inflammatory macrophages (F4/80<sup>+</sup> CD11b<sup>high</sup> cells) and neutrophils (Ly6G<sup>+</sup> Ly6C<sup>-</sup> cells) into the liver as evaluated by flow cytometric analysis (Figure 3E and F). This was associated with less hepatic expression of *Emr1* (encoding for F4/80) and the adhesion molecule *Sele* (encoding for E-SELECTIN) involved in neutrophil recruitment into the liver<sup>38</sup> (Figure 3G). In addition, MCDD-fed *Sh3bp2*<sup>-/-</sup> mice displayed less hepatic inflammation as evaluated by expression of inflammatory markers including *Cd44*, *Tnf*, *Ccl2*, and *Syk* compared with MCDD-fed Wt mice (Figure 3G). This effect of the hepatic inflammation was also confirmed by the decreased hepatic expression of CD44 and SYK at the protein level (Figure 3H) and decreased serum level of CCL2 (Figure 3I). In addition, the hepatic expression of *Trem1*, an important amplifier of TLR4 pathway via SYK activity,<sup>15,23-25</sup> decreased in MCDD-fed *Sh3bp2*<sup>-/-</sup> mice compared with MCDD-fed Wt mice (Figure 3G). In line with this, the expression of *Dap12*, the transmembrane adaptor required for TREM1 function, also decreased (Figure 3G). Because hepatic injury and inflammation are key actors in the fibrogenic process, the 3BP2 deficiency also prevented the priming of hepatic fibrosis as evaluated by the expression of *Tgfb1*, *Timp1*, and *Col1a1* (Figure 3G). The protective effect of 3BP2 deficiency on liver complications was also associated with decreased expression of oxidative stress markers *Cyba* (encoding for P22PHOX) and *heme oxygenase-1* (HMOX1) and increased *Ppar-alpha*, the master regulator of beta-oxidation (Figure 3G). Altogether, we show that by regulating hepatic steatosis, inflammation, and liver injury, 3BP2 plays an important role in the onset of MAFLD.

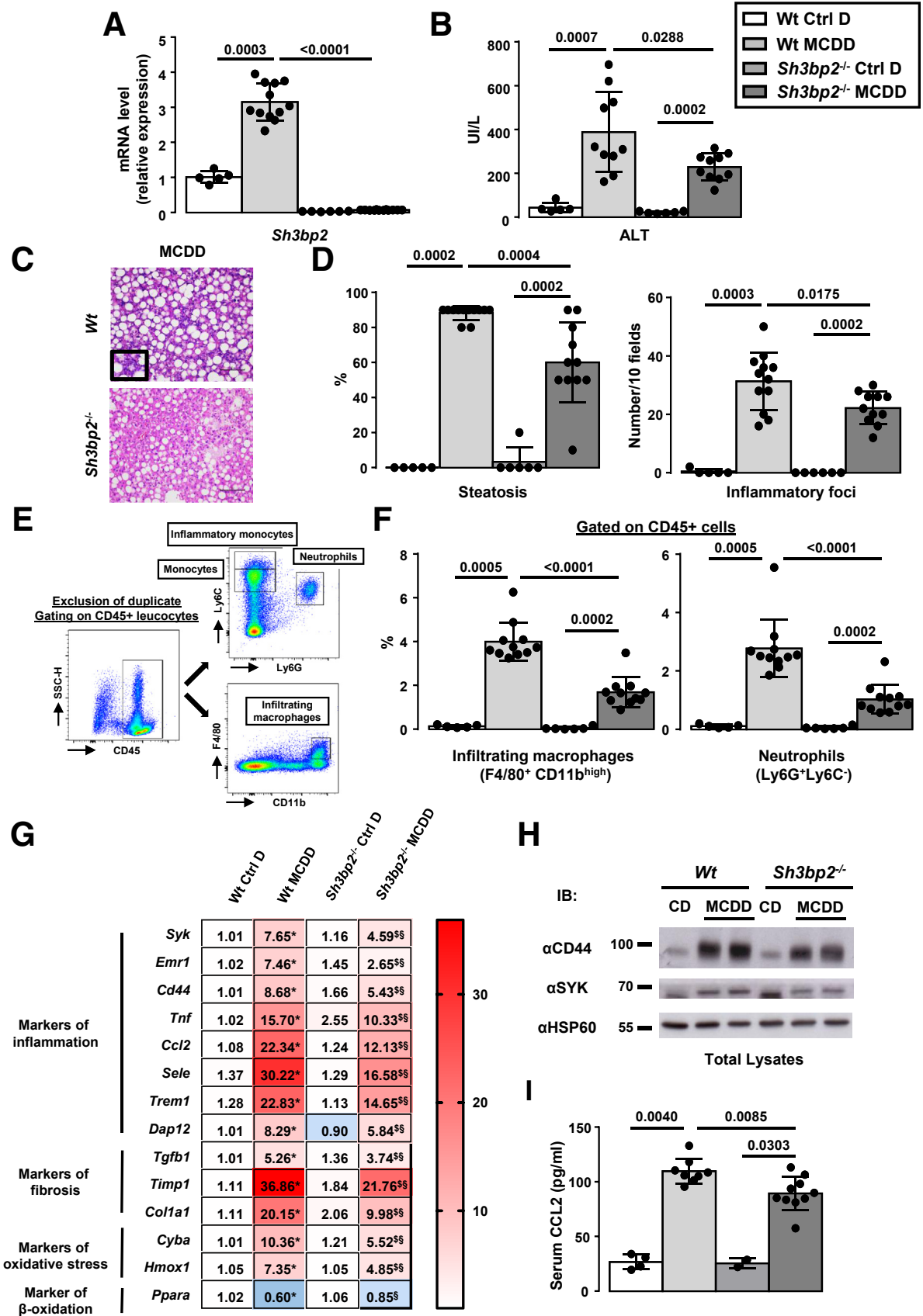
### The SYK/3BP2 Axis Significantly Contributed to the Up-Regulation of Inflammatory Mediators in Lipopolysaccharide-Stimulated Hepatocytes

Because hepatocytes are key actors in the early onset of local inflammation, we investigated the role of 3BP2 and SYK in the expression of inflammatory mediators in hepatocytes. Indeed, hepatocytes sense pathogen products such as lipopolysaccharide (LPS) and contribute to the up-regulation of liver cytokines and chemokines leading to the recruitment of inflammatory cells into the liver.<sup>9</sup> In the steady state, the silencing of *Sh3bp2* strongly decreased the expression of *Syk* in primary mouse hepatocytes. On the other hand, the down-regulation of *Syk* did not impact *Sh3bp2* expression (Figure 4A). In response to LPS, the expression of *Sh3bp2* and *Syk* was up-regulated (LPS vs PBS: *Sh3bp2* = 1.62 ± 0.07, *P* = .0001; *Syk* = 1.54 ± 0.13, *P* = .0074, *n* = 4), and the silencing of *Sh3bp2* prevented LPS-stimulated *Syk* expression (data not shown). In addition, the down-regulation of *Sh3bp2* or *Syk* strongly decreased the up-regulation of inflammatory mediators including *Tnf*, *Ccl2*, *Il1b*, and *Il6* in response to LPS (Figure 4B). In line with this, SYK inhibition by SYK inhibitor R406 (as evaluated by the phosphorylation levels of SYK and ERK) (Figure 4C) strongly prevented the up-regulation of these inflammatory mediators in response to LPS (Figure 4E). Interestingly, R406 treatment also reduced the expression of *Sh3bp2* and *Syk* in the steady state (Figure 4D). These data indicate that 3BP2 regulates SYK expression in challenged hepatocytes and that the SYK/3BP2 axis contributes to the expression of inflammatory mediators in response to PAMPs (LPS).

### The Knockdown of SYK in Myeloid Cells Partially Prevented Liver Injury and Inflammation Induced by MCDD Challenge

We investigated the contribution of SYK to the development of the liver complications mediated by MCDD feeding. Because SYK deficiency leads to perinatal lethality in mice<sup>39,40</sup> and because SYK was preferentially expressed in liver non-parenchymal cells (Figure 2H), we focused on the role of SYK in myeloid cells. The *Syk*<sup>fl<sup>ox</sup>/fl<sup>ox</sup></sup> *LysM*<sup>cre/cre</sup> mice (*mSyk*<sup>KO</sup> mice) displayed a significant decrease in SYK expression in hepatic inflammatory monocytes (Ly6G<sup>-</sup> Ly6C<sup>high</sup> cells) and neutrophils (Ly6G<sup>+</sup> Ly6C<sup>-</sup> cells) without disruption of the SYK expression in lymphocytes as

**Figure 2. (See previous page). Hepatic expression of 3BP2 and SYK correlated with severity of steatohepatitis in mice.** Wild-type mice fed control diet (Ctrl D) or MCDD for 2 and 7 weeks (4–8 mice/group). Serum ALT activity (A) and hepatic steatosis (B) and inflammatory foci accumulation (C) (on H&E stained liver tissue section) have been evaluated. (D) Hepatic expression of *Sh3bp2*, *Syk*, and *Emr1* was evaluated at mRNA level. Gene expression was normalized to mRNA levels of  $\beta 2m$ . Results are expressed relative to expression level in Ctrl D-fed Wt mice for 2 weeks. (E) Correlation between hepatic expression of *Sh3bp2* and *Syk* with hepatic steatosis (%), ALT activity, inflammatory foci number, and hepatic *Emr1* expression were analyzed using Spearman's correlation test. (F) Hepatic expression of *Syk-b* (S) and *Syk* (L) was evaluated at mRNA level in Wt mice fed Ctrl D or MCDD mice for 7 weeks. Gene expression was normalized to  $\beta 2m$  mRNA levels and expressed relative to *Syk-b* (S) level in Ctrl D-fed Wt mice. (G) Hepatic expression of SYK and HSP60 was evaluated at the protein level in mice fed control diet (Ctrl D) or MCDD for 7 weeks (2–4 mice/group). (H) Primary hepatocytes and non-parenchymal cells were isolated from lean mice (*n* = 5). *Sh3bp2* and *Syk* mRNA expression levels were analyzed. Gene expression values were normalized to  $\beta 2m$  mRNA and expressed relative to *Syk* mRNA levels in hepatocytes. (A–D, F, and H) Results are expressed as means ± SD and statistically analyzed using the Mann-Whitney test. \*\**P* < .01 versus control.



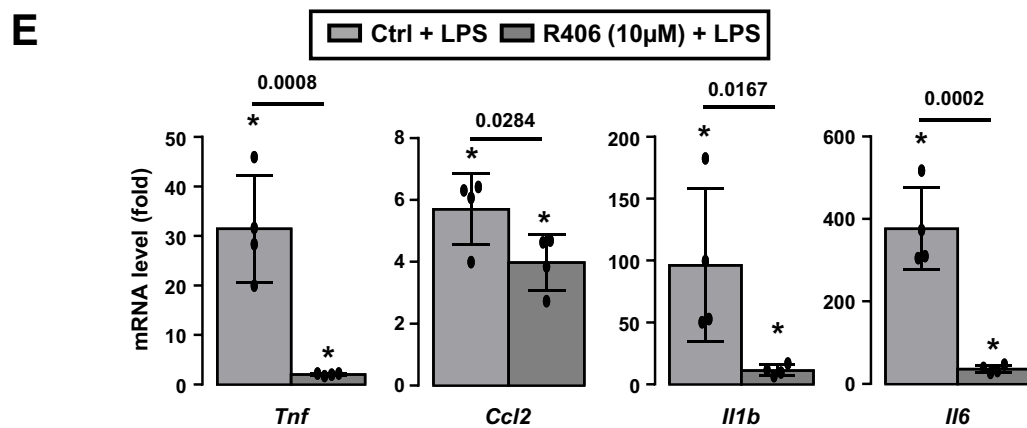
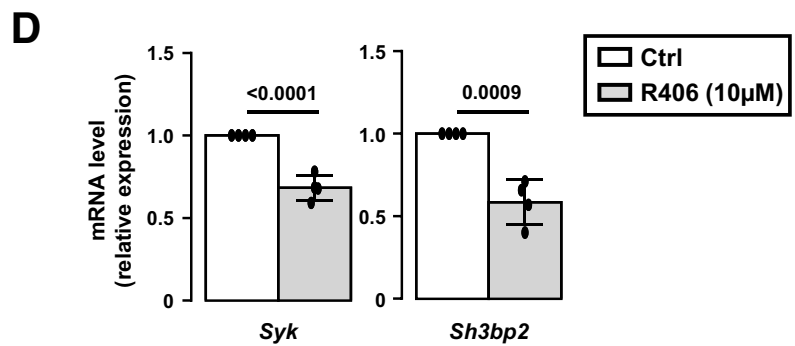
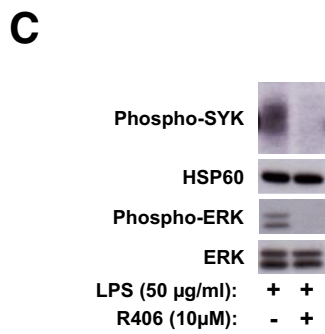
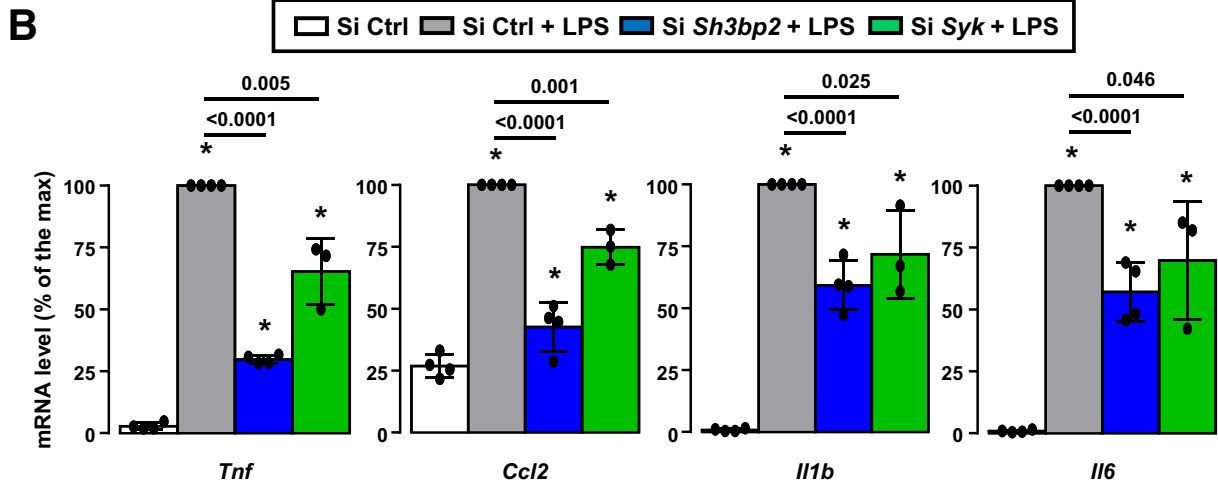
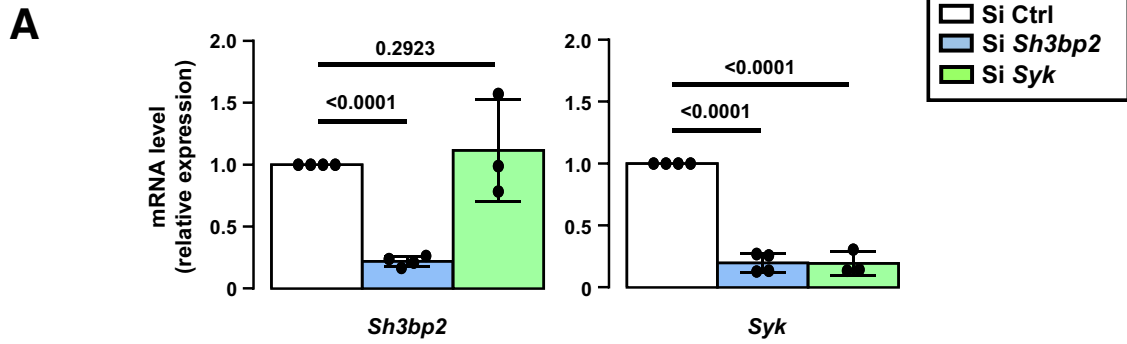
evaluated by flow cytometric analysis (Figure 5A). After 4 weeks of MCDD feeding, the *mSyk*<sup>KO</sup> mice displayed lower hepatic expression of *Syk* than MCDD-fed Wt mice (Figures 5B and H at the gene and protein levels, respectively) without impacting the *sh3bp2* expression level (Figure 5G). In addition, the MCDD-fed *mSyk*<sup>KO</sup> mice exhibited less liver damage, as shown by the lower ALT levels (Figure 5C). Furthermore, histologic analyses showed less accumulation of inflammatory foci in the livers of MCDD-fed *mSyk*<sup>KO</sup> mice compared with livers of MCDD-fed Wt mice without changing in hepatic steatosis (Figure 5D and E). The down-regulation of SYK in myeloid cells strongly prevented the recruitment of infiltrating neutrophils (Ly6G<sup>+</sup> Ly6C<sup>-</sup> cells) and macrophages (F4/80<sup>+</sup> CD11b<sup>high</sup> cells) into the liver (Figure 5F). Moreover, these were associated with reduced hepatic expression of inflammatory markers such as *Cd44* (Figure 5G and H at the gene and protein levels, respectively) and *Sele* (E-Selectin) (Figure 5G). In line with the potential role of SYK in the regulation of macrophage activation/polarization,<sup>18,41</sup> the hepatic expression of M1 markers *Itgax* (CD11C) and *Tnf* decreased, whereas the expression of the M2 marker *Clec10a* (CD301) did not change in MCDD-fed *mSyk*<sup>KO</sup> mice compared with MCDD-fed Wt mice (Figure 5G). As reported for 3BP2 deficiency (Figure 3G), the knockdown of SYK in myeloid cells strongly decreased the hepatic expression of *Trem1* and *Dap12*, the priming of the fibrosis (*Tgfb1* and *Timp1*), and oxidative stress (*Cyba* and *Hmox1*) (Figure 5G). This effect of the inflammation was also confirmed by the decreased serum level of CCL2 (Figure 5I). These results indicate that the conditional ablation of SYK in myeloid cells is sufficient to reduce liver inflammation, injury, and, in turn, the priming of fibrosis in MCDD mice.

### SYK Deletion in Myeloid Cells Prevented Severe Hepatitis and Fibrosis in Homozygous *Sh3bp2*<sup>KI/KI</sup> Mice

To further demonstrate the key role of the SYK/3BP2 pathway in the development of chronic liver diseases, we revisited this pathway in the livers of cherubic mice. Cherubism is an autoinflammatory autosomal dominant bone dysplasia associated with point-mutations of the

*Sh3bp2* gene leading to the accumulation of proteasome-resistant mutant 3BP2. The accumulation of 3BP2 mutant proteins exacerbated activities of intracellular signaling components including SYK in myeloid cells.<sup>31,35,42–44</sup> We evaluated the liver status in homozygous cherubic animals (*Sh3bp2* G418R knock-in mice [*Sh3bp2*<sup>KI/KI</sup> mice], equivalent to the G420R mutation in cherubism patients), which developed systemic inflammation without regression of the lesions with age.<sup>33</sup> The 14-week-old *Sh3bp2*<sup>KI/KI</sup> mice already displayed cherubic manifestation (kyphosis) and facial inflammation (closed eyes) (Figure 6A and B) in addition to elevated liver weight relative to body weight (Figure 6C) and aspartate aminotransferase (AST) to ALT ratio (Figure 6D). We also found that the *Sh3bp2*<sup>KI/KI</sup> mice developed severe hepatitis, as evaluated by the accumulation of large inflammatory foci in the livers without hepatic steatosis (Figure 6E and F). The SYK deletion in myeloid cells in cherubic mice (*mSyk*<sup>KO</sup>*Sh3bp2*<sup>KI/KI</sup> mice) prevented all these clinical and biological abnormalities at the early and late age (mean age, 16- versus 43-week-old mice) (Figure 6A–D, data not shown). Interestingly, the SYK deletion in myeloid cells in *Sh3bp2*<sup>KI/KI</sup> mice decreased the hepatic expression of SYK at the mRNA and protein levels (Figure 6G and H). The SYK deletion in myeloid cells in *Sh3bp2*<sup>KI/KI</sup> mice also prevented hepatic inflammatory foci accumulation even in old mice (Figure 6E and F). This was also associated with lower hepatic expression of macrophage marker *Emr1* and inflammatory markers including *Cd44*, *Tnf*, *Ccl2*, *Trem1*, and *Dap12* (Figure 6G). This effect of inflammation was also confirmed by the decreased hepatic expression of CD44 at the protein level (Figure 6H) and decreased serum level of CCL2 (Figure 6I). In addition to the prevention of liver inflammation, SYK deficiency in myeloid cells was also associated with the prevention of hepatic fibrosis as evaluated by collagen staining (picosirius red stain, Figure 6E) and lower gene expression of fibrosis markers like *Tgfb1*, *Timp1*, and *Col1a1* (Figure 6G). Finally, the hepatic expression of *Sh3bp2* and *Syk* correlated with liver inflammation and fibrosis (Figure 6G). Altogether, we reported that the sustained activation of 3BP2-SYK pathway mediated by 3BP2 G418R mutant is thus associated with the development of significant fibrotic-hepatitis.

**Figure 3. (See previous page). 3BP2 deficiency partially prevented liver injury and steatohepatitis induced by MCDD challenge.** Wt and *Sh3bp2*<sup>-/-</sup> mice fed control diet (Ctrl D) or MCDD for 4 weeks (5–12 mice/group). (A) Hepatic *Sh3bp2* expression was evaluated in Wt Ctrl D and MCDD mice at mRNA level. (B) Serum levels of ALT were evaluated. (C and D) H&E staining of liver tissue sections samples from Wt and *Sh3bp2*<sup>-/-</sup> after MCDD as indicated. Representative images (C) and quantification of hepatic steatosis and inflammatory foci (D) are shown. (E and F) Hepatic non-parenchymal cells were stained for CD45, F4/80, CD11b, Ly6G, and Ly6C and analyzed by flow cytometry (5–11 mice/group). (E) Details regarding the gating strategy for assessment of infiltrating macrophages (F4/80<sup>+</sup> CD11b<sup>high</sup> cells) and neutrophils (Ly6G<sup>+</sup> Ly6C<sup>-</sup> cells) into the liver as evaluated by flow cytometric analysis. (F) Results are expressed as means ± SD and statistically analyzed using the Mann-Whitney test. (G) Hepatic mRNA expression levels of *Syk* and markers of inflammation, fibrosis, oxidative stress, and beta-oxidation were analyzed by real-time quantitative PCR (5–12 mice/group). Data are presented as relative mRNA levels normalized to *B2m* mRNA levels. Data are expressed as means in heat map and statistically analyzed using Mann-Whitney test. \**P* < .05, compared with Wt Ctrl D mice. <sup>§</sup>*P* < .05, compared with *Sh3bp2*<sup>-/-</sup> Ctrl D mice, <sup>§</sup>*P* < .05, compared with Wt MCDD mice. (H) Hepatic expression of CD44, SYK, and HSP60 was evaluated at the protein level in Wt and *Sh3bp2*<sup>-/-</sup> mice fed control diet (Ctrl D) or MCDD for 4 weeks (1–2 mice/group). (I) Serum levels of CCL2 were evaluated (2–10 mice/group). (A, B, D, F, and I) Results are expressed as means ± SD and statistically analyzed using Mann-Whitney test.





### Hepatic Expression of SYK Increased With Metabolic Steatohepatitis in Obese Patients

We examined the relationship between hepatic 3BP2 and SYK expression with MAFLD in human liver biopsies from morbidly obese patients who had undergone bariatric surgery. Patients were classified into 3 groups: without MAFLD, with hepatic steatosis, and with metabolic steatohepatitis and severe steatosis (assessed on the basis of histopathological features; Table 1). Liver mRNA levels of *SH3BP2* did not change with obesity and MAFLD (data not shown). By contrast, liver mRNA levels of *SYK* were strongly up-regulated with metabolic steatohepatitis (Figure 7A). This expression correlated with nonalcoholic fatty liver disease activity score, ALT activity, and hepatic expression of macrophage marker *CD68* (Figure 7B). Consistent with our animal studies, the hepatic expression of SYK could be a local marker of hepatic inflammation in MAFLD patients.

### Discussion

Here we report that hepatic SYK and 3BP2 contribute to the onset of hepatic inflammation by acting on both parenchymal and myeloid cells. In concert with liver macrophages, the SYK/3BP2 axis in hepatocytes could initiate the local inflammation and contribute to the significant accumulation of bone marrow-derived macrophages and neutrophils in the liver, a hallmark of metabolic steatohepatitis and severe hepatitis. Indeed, SYK/3BP2 regulates the LPS-TLR4 pathway in both hepatocytes and macrophages. The genetic deletion of 3BP2 or SYK in a context of metabolic steatohepatitis or deletion of SYK in myeloid cells in a context of a pro-inflammatory 3BP2 mutation significantly reduced liver inflammation, injury, and fibrosis (priming and/or collagen deposition). We also report that hepatic SYK is a marker of liver inflammation and correlates with hepatic macrophage recruitment in mouse and human metabolic steatohepatitis. We also provide evidence that an important mechanism by which 3BP2 participates to metabolic steatohepatitis is the regulation of the expression of its signaling partner SYK, leading to exacerbated SYK-mediated inflammatory pathway in liver. Together, these data provide novel evidence that targeting the SYK/3BP2 axis is a potential therapeutic approach in chronic liver diseases.

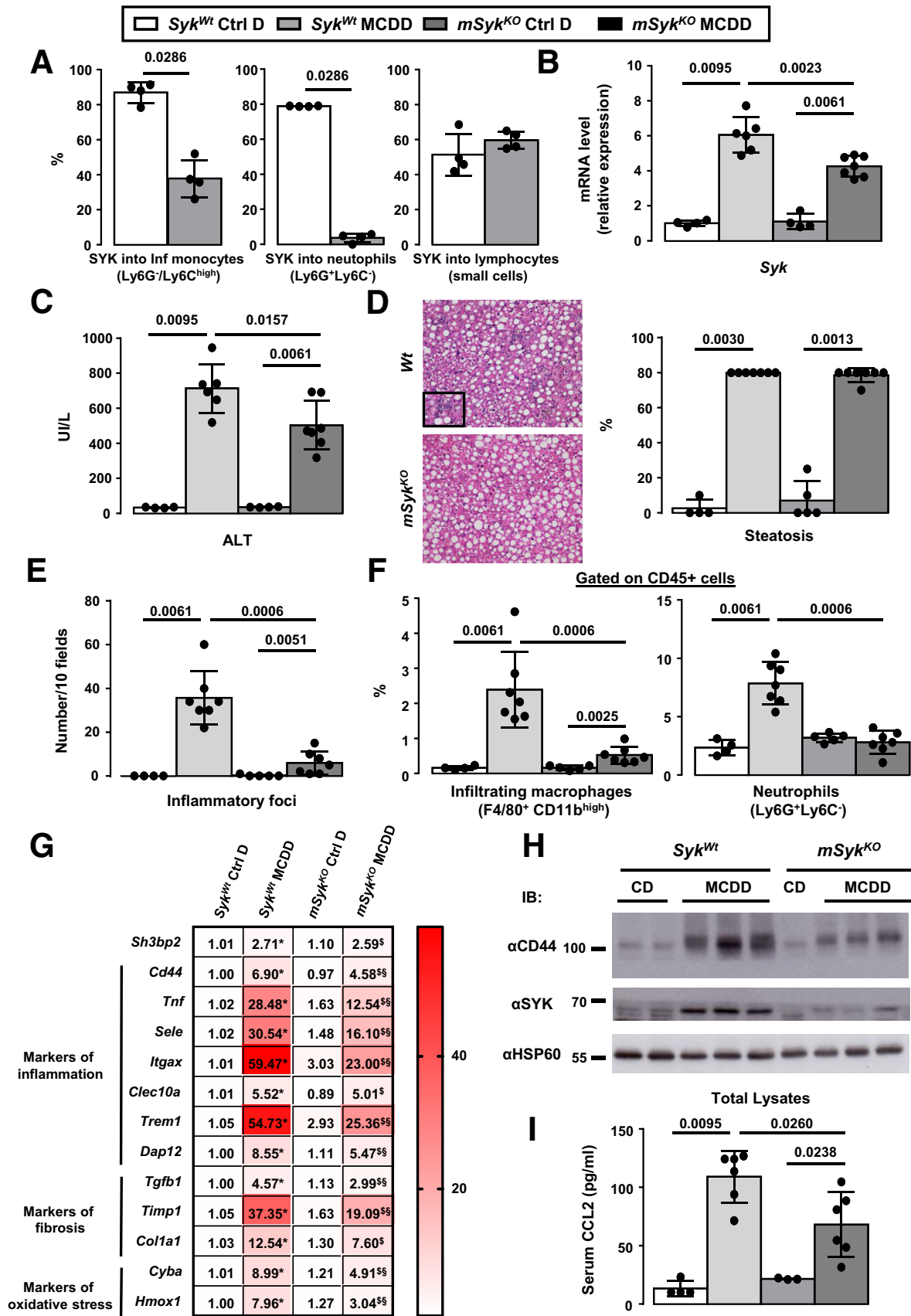
We first show that the SYK/3BP2 pathway in liver parenchymal cells plays an important role in the expression of inflammatory mediators in response to LPS. Remarkably,

3BP2 targeting lowers SYK expression and decreases the expression of tumor necrosis factor (TNF)  $\alpha$ , CCL2, interleukin 1 $\beta$ , and interleukin 6 in response to LPS (Figure 4). Although SYK inhibition slightly decreases the expression of 3BP2, the targeting of SYK (silencing or inhibition) also significantly prevents the up-regulation of these inflammatory mediators upon LPS stimulation (Figure 4). In addition to its detoxifying and metabolic roles, hepatocytes also sense pathogens including bacteria products (for example, LPS) via their membrane and cytoplasmic pattern recognition receptors.<sup>10</sup> Importantly, it has been reported that deficiency or down-regulation of TLR4 in hepatocytes resolved the hepatic inflammation mediated by HFD and associated with decreased insulin resistance, oxidative stress, and hepatic steatosis.<sup>45,46</sup> These studies support the notion that TLR4 signaling in liver parenchymal cells plays a pivotal role during the early stage of MAFLD by initiating local inflammation. Our results emphasize the importance of the hepatocyte SYK/3BP2 signaling pathway to control the LPS/TLR4-mediated responses.

Among the inflammatory mediators, hepatocytes are a source of the chemokine CCL2, whose expression is modulated by the SYK/3BP2 pathway (Figure 4). The CCL2/CCR2 pair is a key player in the recruitment of inflammatory monocytes into the injured liver and drives hepatic fibrosis.<sup>47,48</sup> To illustrate this, it has been reported that pharmacologic inhibition of CCL2 or CCR2 in murine models of MAFLD and chronic liver injury (chronic CCl4 treatment) reduced monocyte recruitment into the liver and ameliorated liver inflammation, injury, and fibrosis.<sup>49,50</sup> Previous studies, including our own, have also reported that hepatic expression of CCL2 was up-regulated in metabolic steatohepatitis patients.<sup>9,51</sup> Therapeutic treatments with a dual antagonist of chemokine receptors CCR2/CCR5 are currently under clinical investigation for patients with fibrotic metabolic steatohepatitis.<sup>9</sup>

This indicates that regulation of the influx of bone marrow-derived monocytes into the liver is an important event in the onset of liver inflammation and MAFLD progression.<sup>9,49,52</sup> In addition to therapeutic chemokine targeting, we show here that global deficiency of 3BP2 and SYK deletion in myeloid cells both prevent the recruitment of macrophages and neutrophils into the liver associated with reduced hepatic expression of CCL2 but also CD44 and E-selectin (Figures 3 and 5). CD44 and E-selectin (CD62E) are also important drivers of leukocyte recruitment into the inflamed liver,<sup>9</sup> and we have previously demonstrated that

**Figure 4.** (See previous page). 3BP2/SYK pathway contributed to expression of inflammatory mediators in LPS-stimulated hepatocytes. (A and B) Primary mouse hepatocytes were transfected with Si Ctrl (n = 4), Si Sh3bp2 (n = 4), or Si Syk (n = 3) for 48 hours as indicated. Cells were then incubated with medium supplemented with 0.5% bovine serum albumin for 1 hour and treated with LPS (50  $\mu$ g/mL) or phosphate-buffered saline for 6 hours. (C) Primary mouse hepatocytes were incubated overnight with medium supplemented with 0.5% bovine serum albumin and then successively treated with R406 (10  $\mu$ mol/L) for 2 hours and LPS (50  $\mu$ g/mL) for 5 minutes (representative immunoblots are shown). (D and E) Primary mouse hepatocytes were incubated with medium supplemented with 0.5% bovine serum albumin without or with R406 (10  $\mu$ mol/L) for 1 hour and then treated with LPS (50  $\mu$ g/mL) or phosphate-buffered saline for 6 hours. (A, B, D, and E) *Sh3bp2*, *Syk*, *Tnf*, *Ccl2*, *Il1b*, and *Il6* mRNA expression levels were analyzed by real-time quantitative PCR as indicated. Gene expression values were normalized to *Rplp0* mRNA levels. Results are expressed as means  $\pm$  SD. Data were statistically analyzed using Student *t* test. \**P* < .05 versus Si Ctrl or Ctrl.



their hepatic expression was strongly up-regulated in metabolic steatohepatitis patients.<sup>51,53</sup> From our experimental data, we also found that CD44, which interacts with extracellular matrix components including E-selectin, regulates the recruitment of macrophages and neutrophils into the liver. CD44 also regulates the macrophage activation mediated by TLR4 ligands including DAMPs, LPS, and saturated fatty acids in a context of steatohepatitis.<sup>53</sup> This pro-inflammatory polarization of resident and recruited liver myeloid cells can also be dependent on the SYK/3BP2 pathway. Indeed, we have recently reported that 3BP2 is necessary for LPS-induced activation of signaling pathways in macrophages.<sup>27–29,31</sup> In addition, it has been shown that SYK inhibition prevents the pro-inflammatory polarization of macrophages.<sup>41</sup> An important additional amplifier of TLR4-mediated hepatic inflammation is the TREM1/DAP12 pathway.<sup>23–25</sup> Interestingly, we here report that the prevention of liver inflammation and injury mediated by the targeting of 3BP2 or SYK strongly decrease TREM1/DAP12 expression. Because of the central place of the SYK pathway in both TLR4 and TREM-1 signaling,<sup>23</sup> this suggests the establishment of an inflammatory loop in which SYK and its partner 3BP2 exacerbate liver inflammation.

The chronicity of liver inflammation is also an important driver of the progression of liver complications such as liver injury and fibrosis. From our different mouse models, the down-regulation of 3BP2 or SYK in myeloid cells reduces both liver injury and fibrosis (fibrosis priming and/or collagen accumulation) along with significant decrease in hepatic inflammation (Figures 3, 5, and 6). In line with these results, SYK deletion in the myeloid compartment confers protection against fibrogenic progression upon TAA-mediated liver injury.<sup>18</sup> Of the mechanisms related to liver injury, TNF- $\alpha$  and sustained oxidative stress are reported to mediate hepatocyte death in chronic liver and inflammatory diseases.<sup>51,54,55</sup> Interestingly, 3BP2 and SYK mutant mice display a reduction in liver expression of TNF- $\alpha$  and markers of oxidative stress (P22phox and Ho-1), coupled with reduced liver injury (Figures 3 and 5). In addition to promoting liver inflammation and associated injury, the SYK pathway can also directly regulate the activity of the HSC. Indeed, it has been shown that SYK inhibitors prevented HSC activation *in vitro* and in animal models of hepatic fibrosis.<sup>17,18</sup> However, the protective effects of SYK targeting seem to be more related to an effect on myeloid cells than

on HSC because its deficiency in HSC (Lrat<sup>Cre</sup>Syk<sup>flox/flox</sup>) did not mitigate the severity of fibrosis mediated by TAA treatment.<sup>18</sup>

Interestingly, we also show that SYK deletion in myeloid cells prevents hepatic inflammation in cherubic mice expressing the 3BP2 G418R mutant (Sh3bp2 G418R knock-in mice, equivalent to the G420R mutation in cherubism patients). Indeed, SYK deletion in these mice mediates a drastic reduction in inflammatory foci number, macrophage recruitment, and hepatic expression of TNF- $\alpha$ , CCL2, and CD44. These protective mechanisms were also associated with restoration of hepatic 3BP2 and SYK expression to normal in Sh3bp2 G418R knock-in mice (Figure 6). Interestingly, both the protective effects of SYK deletion in the accumulation of inflammatory foci and the up-regulation of hepatic TNF- $\alpha$  expression have been recently reported in another mouse model of cherubic mice (Sh3bp2 P416R knock-in mice).<sup>36</sup> We further show in our Sh3bp2 G418R knock-in mice that the selective knockdown of SYK in myeloid cells is also sufficient to prevent the development of liver fibrosis with the quasi-absence of collagen deposition and changes to TGF $\beta$ , TIMP1, and COL1 $\alpha$ 1 expression (Figure 6). Because the SYK inhibitor treatment in cherubic mice reduces systemic and hepatic inflammation,<sup>37</sup> the inhibition of SYK activity could also ameliorate liver fibrosis in mouse cherubism.

We also report that the 3BP2 deficiency reduces liver steatosis upon MCDD challenge (Figure 3). Although additional studies to better understand the role of 3BP2 in hepatocyte metabolism and steatosis development are needed, the 3BP2 deficiency is associated with the prevention of decreased peroxisome proliferator activated receptor alpha (PPAR $\alpha$ ) upon MCDD challenge (Figure 3G). It is well-established that PPAR $\alpha$  plays a key role in the regulation of hepatocyte metabolism including fatty acid uptake, beta-oxidation, and triglyceride turnover.<sup>56</sup> Mice with genetic deletion of PPAR $\alpha$  fed MCDD developed more severe steatosis and necroinflammation compared with Wt mice. To the contrary, treatment with PPAR $\alpha$  agonist Wy-14643 can prevent and reverse MCDD-induced hepatic steatosis, inflammation, and liver injury in a PPAR $\alpha$ -dependent manner, likely via increased fatty acid oxidation.<sup>57,58</sup> Interestingly, the treatment of primary hepatocytes with the SYK inhibitor R406 also enhances PPAR $\alpha$  and PGC1 $\alpha$  expression (Ppara:  $\times 1.8 \pm 0.2$ ,  $P = .029$ ; Pgc1a:  $\times 4.6 \pm 1.0$ ,  $P = .013$ ,

**Figure 5. (See previous page). SYK deletion in myeloid cells partially prevented liver injury and inflammation induced by MCDD challenge.** Wild-type (Syk<sup>Wt</sup>) and Syk<sup>flox/flox</sup> LysM<sup>cre/cre</sup> (*mSyk*<sup>KO</sup>) mice fed control diet (Ctrl D) or MCDD for 4 weeks (4–7 mice/group). (A) Evaluation of SYK expression in hepatic inflammatory monocytes (Ly6G<sup>-</sup> Ly6C<sup>high</sup> cells), neutrophils (Ly6G<sup>+</sup> Ly6C<sup>-</sup> cells), and lymphocytes (small cells) by flow cytometric analysis (4 mice/group). (B and G) Hepatic mRNA expression levels of *Syk*, *Sh3bp2*, and markers of inflammation, fibrosis, and oxidative stress were analyzed by real-time quantitative PCR (4–7 mice/group). Data are presented as relative mRNA levels normalized to  $\beta 2m$  mRNA levels. Data are expressed as means  $\pm$  SD (B) or as means in heat map (G) and statistically analyzed using Mann-Whitney test. \* $P < .05$ , compared with Syk<sup>Wt</sup> Ctrl D mice.  $^{\$}P < .05$ , compared with *mSyk*<sup>KO</sup> Ctrl D mice.  $^{\$}P < .05$ , compared with Syk<sup>Wt</sup> MCDD mice. (C) Serum levels of ALT were evaluated. (D) H&E staining of liver tissue sections from Syk<sup>Wt</sup> and *mSyk*<sup>KO</sup> after MCDD as indicated. Representative pictures and quantification of hepatic steatosis are shown. (E) Quantification of inflammatory foci. (F) Liver non-parenchymal cells were stained for CD45, F4/80, CD11b, Ly6G, and Ly6C and analyzed by flow cytometry (4–7 mice/group). (H) Hepatic expression of CD44, SYK, and HSP60 was evaluated at the protein level in Syk<sup>Wt</sup> and *mSyk*<sup>KO</sup> mice fed control diet (Ctrl D) or MCDD for 4 weeks (1–3 mice/group). (I) Serum levels of CCL2 were evaluated (3–6 mice/group). (A–F and I) Results are expressed as means  $\pm$  SD and statistically analyzed using Mann-Whitney test.

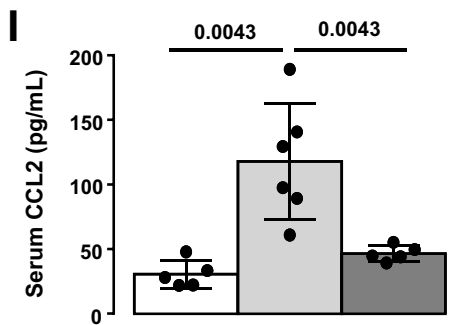
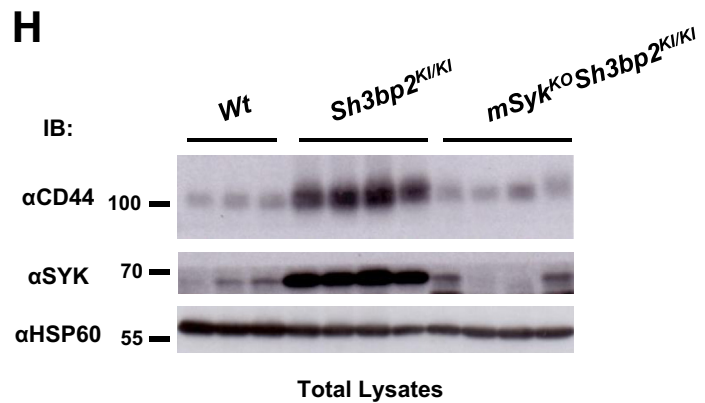
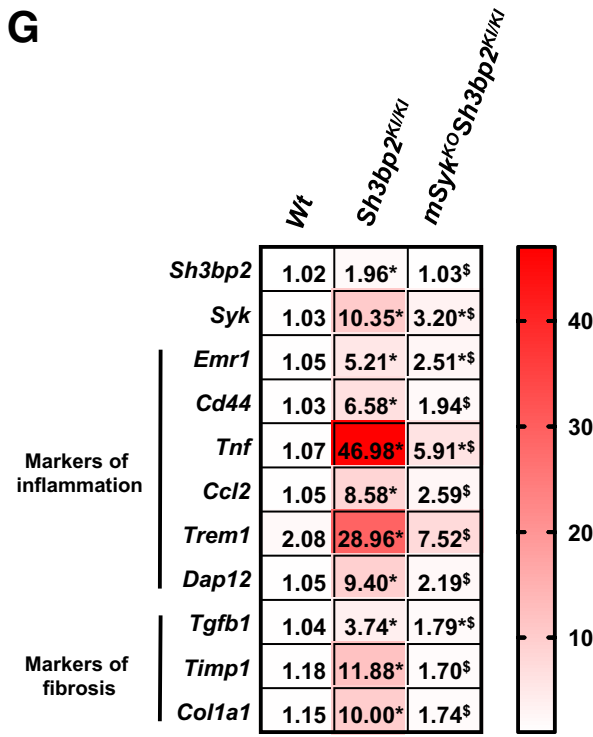
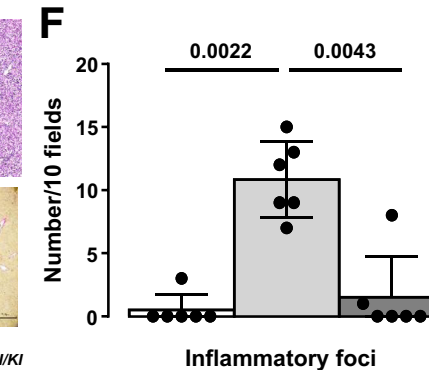
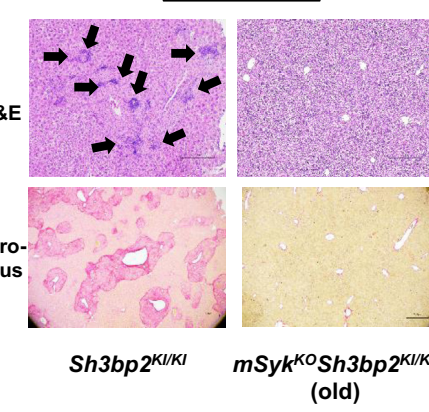
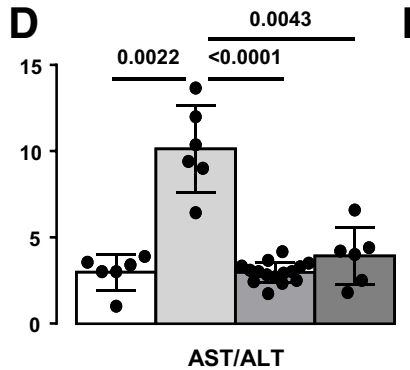
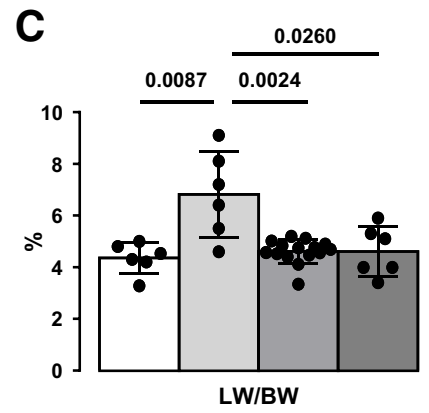
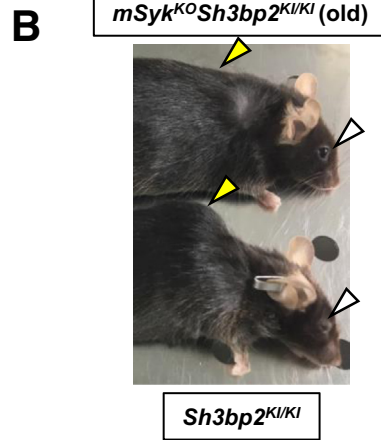
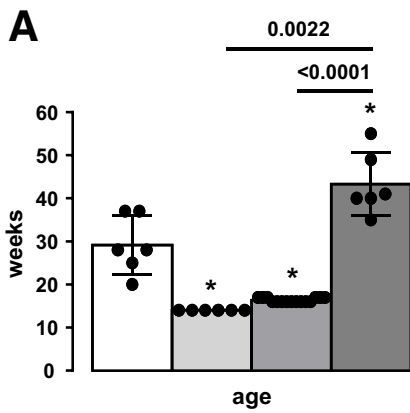
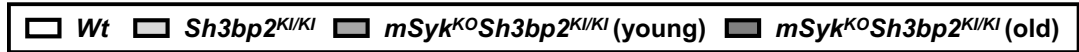


**Table 1.** Characteristics of the Obese Patients

	Without MAFLD	Steatosis	NASH
n	6	16	11
Age (y)	37.8 ± 12.7	36.6 ± 9.2	42.5 ± 10.3
BMI (kg/m <sup>2</sup> )	42.9 ± 1.1	43.2 ± 4.4	44.6 ± 6.1
ALT (IU/L)	14.0 ± 3.6	31.8 ± 10.9 <sup>a</sup>	94.6 ± 78.6 <sup>a,b</sup>
AST (IU/L)	18.1 ± 4.3	23.4 ± 5.4 <sup>a</sup>	59.1 ± 43.1 <sup>a,b</sup>
Fasting insulin (mIU/L)	11.1 ± 7.4	15.7 ± 12.0	39.3 ± 28.5 <sup>a,b</sup>
Fasting glucose (mmol/L)	4.8 ± 0.3	5.3 ± 0.5 <sup>a</sup>	7.9 ± 4.5 <sup>a</sup>
HOMA-IR	2.3 ± 1.3	3.8 ± 3.0	13.3 ± 10.8 <sup>a,b</sup>
Hemoglobin A1c (%)	5.2 ± 0.4	5.6 ± 0.4	6.8 ± 1.7 <sup>a,b</sup>
NAFLD activity score (n)	0 (6)	1 (1) 2 (5) 3 (10)	5 (11)
Grade of steatosis (n)	0 (6)	1 (1) 2 (6) 3 (9)	3 (11)
Lobular inflammation (n)	0 (6)	0 (15) 1 (1)	1 (11)
Hepatocellular ballooning (n)	0 (6)	0 (16)	1 (11)

NOTE. Without MAFLD: patients with normal liver histology; Steatosis: patients with steatosis; NASH: patients with severe steatosis and nonalcoholic steatohepatitis. Data are expressed as mean ± SD and compared using the non-parametric Mann-Whitney test.

BMI, body mass index; HOMA-IR, homeostatic model assessment for insulin resistance.

<sup>a</sup>P < .05 compared with “Without MAFLD”.

<sup>b</sup>P < .05 compared with “Steatosis”.

n = 4). Altogether, this suggests that SYK and its signaling partner 3BP2 could also be important regulators of hepatocyte metabolism and liver steatosis development.

Finally, we find that the hepatic expression of SYK is up-regulated with metabolic steatohepatitis and correlates with the presence of liver macrophage in obese patients (Figure 7). This is not dependent on hepatic fibrosis because our patients with liver biopsy-proven steatosis or metabolic steatohepatitis have only minimal scarring (F1: portal fibrosis without septa). Interestingly, different groups recently reported an association between the hepatic levels of SYK and liver fibrosis/cirrhosis in patients with hepatitis B virus infection, hepatitis C virus infection, alcohol abuse, cholestasis, and metabolic steatohepatitis.<sup>17,41,59</sup> Altogether, these results could indicate that liver SYK expression is a relevant new biomarker for metabolic steatohepatitis and its progression to cirrhosis.

In summary, the harmful functions of the SYK/3BP2 signaling pathway in chronic liver diseases occur at different stages of the disease (from steatosis to fibrosis)

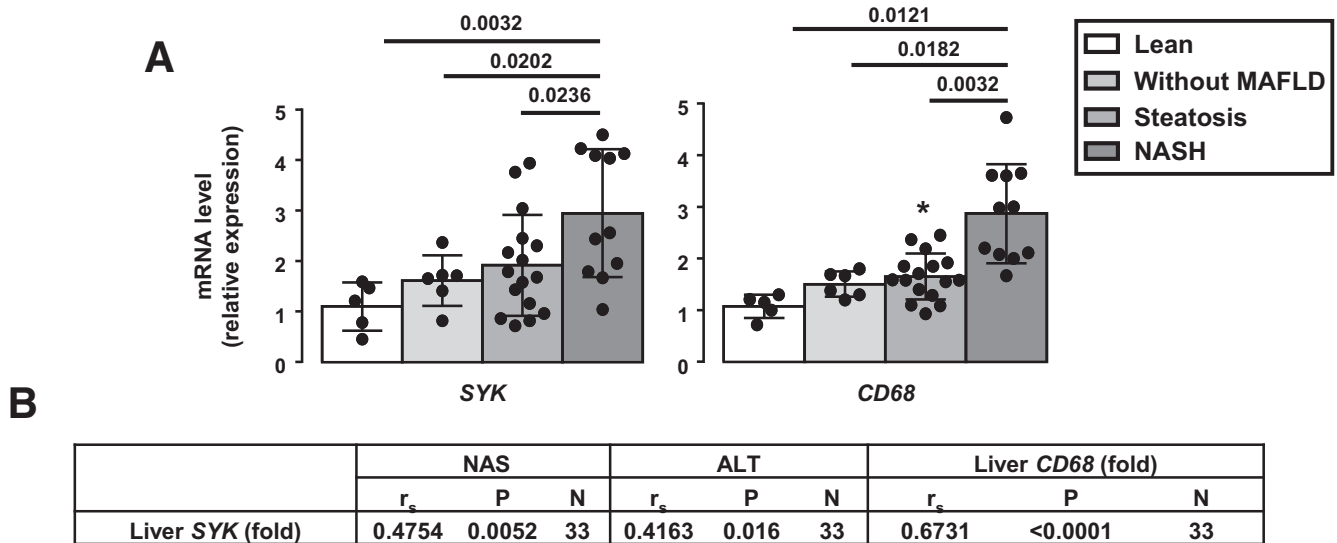
and in different liver cells (hepatocytes, macrophages, HSC, etc). In the early stages by enhancing LPS-TLR4 responses in hepatocytes and resident macrophages, the SYK/3BP2 pathway could initiate the onset of local inflammation and the up-regulation of factors involved in the recruitment of monocytes and neutrophils into the liver. The increase in pro-inflammatory polarization of recruited macrophages by SYK and 3BP2 could fuel a feed-forward mechanism whereby the amplified local inflammation subsequently contributes to liver injury and fibrosis. Inhibition of the SYK/3BP2 pathway in both hepatocytes and liver non-parenchymal cells (macrophages and HSCs) could represent a new therapeutic strategy to dampen inflammation, cell death, and disease progression in chronic liver diseases.

## Materials and Methods

### Animals and Study Design

**Transgenic mice.** Mice had a C57BL/6 background. *Sh3bp2*<sup>-/-</sup> (*Sh3bp2*<sup>KO</sup>) mice have previously been

**Figure 6. (See previous page).** SYK deletion in myeloid cells prevented severe hepatitis in homozygous *Sh3bp2*<sup>KI/KI</sup> mice. Wild-type (mean age = 29 weeks, n = 6, 16% of male), *Sh3bp2*<sup>KI/KI</sup> (mean age = 14 weeks, n = 6, 33% of male), young *mSyk*<sup>KO</sup> *Sh3bp2*<sup>KI/KI</sup> (mean age = 16 weeks, n = 15, 58% of male), and old *mSyk*<sup>KO</sup> *Sh3bp2*<sup>KI/KI</sup> (mean age = 43 weeks, n = 6, 50% of male) mice were characterized. (A) Age of the mice. (B) Facial appearance (white arrows) (open eyelids reflect lack of facial inflammation) and kyphosis (yellow arrows) of 14-week-old *Sh3bp2*<sup>KI/KI</sup> mice and 41-week-old *mSyk*<sup>KO</sup> *Sh3bp2*<sup>KI/KI</sup> mice are shown. (C) Liver to body weight. (D) Serum AST/ALT ratio. (E) H&E and picrosirius red staining of liver samples from *Sh3bp2*<sup>KI/KI</sup> and old *mSyk*<sup>KO</sup> *Sh3bp2*<sup>KI/KI</sup> mice as indicated. Representative pictures are shown. (F) Quantification of inflammatory foci. (G) Hepatic mRNA expression levels of *Syk*, *Sh3bp2*, and markers of inflammation (*Emr1*, *Cd44*, *Tnf*, *Ccl2*, *Trem1*, *Dap12*) and fibrosis (*Tgfb1*, *Timp1*, and *Col1a1*) were analyzed by real-time quantitative PCR (6 mice/group). Data are presented as relative mRNA levels normalized to  $\beta 2m$  mRNA levels. Data are expressed as means in heat map and statistically analyzed using Mann-Whitney test. \*P < .05, compared with Wt mice. <sup>§</sup>P < .05, compared with *Sh3bp2*<sup>KI/KI</sup> mice. (H) Hepatic expression of CD44, SYK, and HSP60 was evaluated at the protein level in Wt, *Sh3bp2*<sup>KI/KI</sup>, and old *mSyk*<sup>KO</sup> *Sh3bp2*<sup>KI/KI</sup>. (F) Serum levels of CCL2 were evaluated (5–6 mice/group). (A, C, D, F, and I) Results are expressed as means ± SD and statistically analyzed using Mann-Whitney test.



Spearman's rank correlation test.

**Figure 7. Hepatic SYK expression increased with metabolic steatohepatitis in obese patients.** (A) Liver SYK and CD68 mRNA expression levels were analyzed by real-time quantitative PCR in lean patients ( $n = 5$ ), in severely obese patients without MAFLD ( $n = 6$ ), with hepatic steatosis ( $n = 16$ ), and with severe hepatic steatosis and metabolic steatohepatitis ( $n = 11$ ). Gene expression values were normalized to *RPLP0* mRNA levels. Results are expressed relative to expression level in lean subjects (means  $\pm$  SD) and statistically analyzed using Mann-Whitney test. (B) Correlation between hepatic SYK expression (fold change) with nonalcoholic fatty liver disease activity score (NAS), ALT activity, and hepatic expression of CD68 (fold change) were analyzed using Spearman's correlation test. NASH, nonalcoholic steatohepatitis.

described.<sup>60</sup> *Sh3bp2*<sup>KI/KI</sup> <sup>31</sup> were generated by the Institut Clinique de la Souris (Illkirch, France, <http://www-mci.u-strasbg.fr>) by knocking-in a GGA-to-CGA mutation in the *Sh3bp2* exon 9, resulting in a Gly418-to-Arg substitution in 3BP2 protein, as previously described.<sup>31</sup> *LysM*<sup>cre/cre</sup> (B6.129P2-Lyz2<sup>tm1(cre)lfo</sup>/J) mice were provided by the Jackson Laboratory (Bar Harbor, ME). The *Syk* conditional knockout mouse (*Syk* cKO) model was generated by the Institut Clinique de la Souris (internal reference IR00002283/K504) by floxing exon 2 (containing the ATG starting site) and exon 3 of the *Syk* locus. Myeloid *Syk* conditional mutant mice (*mSyk*<sup>KO</sup>) were obtained by crossing the *Syk* cKO strain with the *LysM*<sup>cre/cre</sup> transgenic mice

**HFD.** Seven-week-old Wt mice (Janvier Labs, Le Genest-Saint-Isle, France) were acclimated to our animal facilities under a 12-hour/12-hour light/dark cycle at a temperature of 21°C  $\pm$  2°C and were fed ad libitum either a HFD (45% fat D12451; Research Diet, New Brunswick, NJ) or control diet (Ctrl D) for 33 weeks.

**MCDD.** Averaging 19-week-old male Wt, *Sh3bp2*<sup>KO</sup> and *Syk*<sup>Flox/Flox</sup>*LysM*<sup>cre/cre</sup> (*mSyk*<sup>KO</sup>) C57BL/6 male mice were acclimated to our animal facilities under 12-hour/12-hour light/dark cycle at a temperature of 21°C  $\pm$  2°C and were fed ad libitum either MCDD or control diet (Ctrl D) for 2, 4, and 7 weeks as indicated (diets from SSMIFF (MCDD # E15653-94; control diet # E15654-04).

**Characterization of *Sh3bp2*<sup>KI/KI</sup> mice.** Wt (mean age, 29 weeks,  $n = 6$ , 16% of male), *Sh3bp2*<sup>KI/KI</sup> (mean age, 14 weeks,  $n = 6$ , 33% of male), young *mSyk*<sup>KO</sup> *Sh3bp2*<sup>KI/KI</sup>

(mean age, 16 weeks,  $n = 15$ , 58% of male), and old *mSyk*<sup>KO</sup> *Sh3bp2*<sup>KI/KI</sup> (mean age, 43 weeks,  $n = 6$ , 50% of male) were analyzed. At the end of the corresponding challenge, blood was collected, and mice were immediately killed, after which the liver was removed. One part of the liver was immediately frozen in liquid nitrogen and stored at -80°C until analysis. The second part was fixed in buffered formalin, paraffin-embedded, sectioned, and stained with hematoxylin-eosin and picosirius red as indicated. The remaining part was used for a flow cytometry analysis. The guidelines of laboratory animal care were followed, and the local ethical committee approved the animal experiments (Comité Institutionnel d'Ethique Pour l'Animal de Laboratoire, national agreement no. 28) (NCE/2013-108) (mouse models of MAFLD: APAFIS#5100-2015121110477413 v6) (*Sh3bp2* project: APAFIS#6999-2016110416248139 v3) (*SYK* project: APAFIS#16775-2018090516097783 v2) (Authorization of the C3M animal facility: B06-088-20).

### Human Samples

Morbidly obese patients (Nice) (gene expression:  $n = 33$ ) were recruited through the Department of Digestive Surgery and Liver Transplantation (Archet 2, University Hospital, Nice, France) where they underwent bariatric surgery for their morbid obesity. Bariatric surgery was indicated for these patients in accordance with French guidelines. Exclusion criteria were presence of hepatitis B or hepatitis C infection, excessive alcohol consumption (>20 g/d), or another cause of chronic liver disease as

previously described.<sup>53,61,62</sup> The characteristics of the study groups are described in [Table 1](#). Before surgery, fasting blood samples were obtained and used to measure ALT and AST, glucose, insulin, and hemoglobin A1c. Insulin resistance was calculated using the homeostatic model assessment index.<sup>63</sup> Surgical liver biopsies were obtained during surgery, and no ischemic preconditioning was performed. Hepatic histopathological analysis was performed according to the scoring system of Kleiner et al.<sup>64</sup> Three histopathological features were semiquantitatively evaluated: grade of steatosis (0, <5%; 1, 5%–30%; 2, >30%–60%; 3, >60%), lobular inflammation (0, no inflammatory foci; 1, <2 inflammatory foci per ×200 field; 2, 2–4 inflammatory foci per ×200 field; 3, >4 inflammatory foci per ×200 field), and hepatocellular ballooning (0, none; 1, few balloon cells; 2, many cells/prominent ballooning). Nonalcoholic fatty liver disease activity score, which is the unweighted sum of scores of steatosis, lobular inflammation, and hepatocellular ballooning, was used to grade activity. Presence of metabolic steatohepatitis was defined as nonalcoholic fatty liver disease activity score  $\geq 5$ .

### Control Subjects

Liver tissue was obtained from 5 lean subjects (5 women; age,  $44 \pm 9$  years; body mass index,  $21 \pm 1.9$  kg/m<sup>2</sup>) undergoing partial hepatectomy for benign tumors (neighbor tissues from 4 adenoma and 1 focal nodular hyperplasia; CHU Henri Mondor, Department of Pathology, AP-HP - Université Paris Est Créteil, Créteil, France). Three subjects underwent left lobectomy or bisegmentectomy without ischemic preconditioning, and 2 patients underwent right hepatectomy with potential ischemic preconditioning (no data). Liver samples did not display any hepatic steatosis, inflammation, or fibrosis. All subjects gave their informed written consent to participate in this study in accordance with French legislation regarding Ethics and Human Research (Huriet-Serusclet law). The Comité Consultatif de Protection des Personnes dans la Recherche Biomédicale de Nice approved the study (07/04:2003, N° 03.017).

### Serum Transaminases Assay and CCL2 Levels

Serum transaminases activity (AST/ALT) was determined using an in vitro test with pyridoxal phosphate activation on Roche/Hitachi cobas c systems (ASTPM, ALTPM; cobas, Meylan, France). Roche/Hitachi cobas c systems automatically calculate the concentration of each sample. Serum levels of CCL2 were evaluated with enzyme-linked immunosorbent assay (#DY479; Bio-Techne, Minneapolis, MN), as described in the manufacturer's instructions (dilution to the fifth).

### Flow Cytometric Analysis

A fraction of the mouse liver was crushed on a 100  $\mu$ m cell strainer and washed with RPMI 1640 medium. The cellular suspension was centrifuged at 630g for 5 minutes at 4°C. The cell pellet was resuspended and centrifuged on a density cushion of Percoll (40% and 70%) at 780g for 20

minutes at room temperature. The non-parenchymal cell fraction between 40% and 70 % Percoll was collected, centrifuged at 630g for 5 minutes at 4°C, and resuspended in phosphate-buffered saline containing 3% fetal bovine serum and 5 mmol/L EDTA. Cell suspensions were incubated with purified anti-FcγRII/III monoclonal antibody blocking antibody before being stained at 4°C for 10 minutes to block Fc receptors. Cells were then stained with fluorochrome-coupled antibodies for 30 minutes at 4°C against CD45 (clone 30F11), F4/80 (clone BM8), CD11b (clone M1/70), Ly6G (clone 1A8), or Ly6C (clone AL21). All antibodies were purchased from BD Biosciences (Franklin Lakes, NJ), eBioscience (San Diego, CA), and Bio Rad ABD Serotec (Oxford, United Kingdom). For intracellular staining, cells were fixed and permeabilized using the BD Cytofix/Cytoperm (Ref 554714) according to the manufacturer's instructions. Samples were first stained for cell surface markers as described above and then for intracellular markers using anti-SYK antibodies (clone D3Z1E XP, PE conjugate; Cell Signaling Technology, Danvers, MA). Samples were acquired using a fluorescence activated cell sorting (FACS) Canto II flow cytometer, and the data were analyzed using the FACS Diva software version 8.0.1 (BD Biosciences) or FlowJo V10 software (Treestar, Ashland, OR).

### Hepatic Parenchymal and Non-parenchymal Cell Isolation

Mouse hepatocytes were isolated with a two-step collagenase procedure. Briefly, mouse livers were perfused with HEPES buffer containing 8 g/L NaCl, 33 mg/L Na<sub>2</sub>HPO<sub>4</sub>, 200 mg/L KCl, and 2.38 g/L HEPES, pH 7.5, supplemented with 0.5 mmol/L EGTA for 3 minutes at 3 mL/min, then with HEPES buffer for 3 minutes at 3 mL/min, and finally with HEPES buffer supplemented with 1.5 g/L CaCl<sub>2</sub> and 0.026% collagenase type IV (Sigma-Aldrich; C5138, Saint-Quentin-Fallavier, France) for 7 minutes at 3 mL/min. Livers were then carefully removed and minced in Williams' E medium (Thermo Fisher Scientific Inc, Waltham, MA) supplemented with 10% fetal bovine serum (Thermo Fisher Scientific Inc), 100 units/mL penicillin, 100 mg/mL streptomycin, 2 mmol/L L-glutamine, and 0.02 UI/mL insulin (Umulin; Lilly France, Neuilly-sur-Seine, France). The cell suspension was then filtered (100  $\mu$ m), and hepatocytes were pelleted after 2 centrifugations at 50g for 5 minutes. The supernatants were collected at each step, which contained the non-parenchymal cell fraction. Pelleted hepatocytes were resuspended in 39% Percoll solution, centrifuged at 50g for 5 minutes at room temperature, and collected at the bottom of the tube. Viability was evaluated by trypan blue exclusion (Sigma-Aldrich).

### Primary Hepatocyte Treatments

Down-regulation of 3BP2 and SYK was achieved using Lipofectamine RNAiMAX technologies (MSS216132, Mouse Sh3bp2; HSS238073, mouse Syk; Life Technologies, Carlsbad, CA) according to the manufacturer's instructions. After 48-hour transfection, cells were incubated with Williams' E medium supplemented with 0.5% bovine serum albumin for

1 hour and then treated with LPS (50  $\mu\text{g}/\text{mL}$ ) for 6 hours. For the R406 inhibitor, cells were incubated with (1) Williams' E medium supplemented with 0.5% bovine serum albumin overnight and then successively treated with R406 (10  $\mu\text{mol}/\text{L}$ ) for 2 hours and then LPS (50  $\mu\text{g}/\text{mL}$ ) for 5 min as indicated (Western blot analysis) and (2) Williams' E medium supplemented with 0.5% bovine serum albumin without or with R406 (10  $\mu\text{mol}/\text{L}$ ) for 1 hour and then treated with LPS (50  $\mu\text{g}/\text{mL}$ ) for 6 hours (gene expression analysis).

### Real-Time Quantitative Polymerase Chain Reaction Analysis

Total liver RNA was extracted using the RNeasy Mini Kit (74104; Qiagen, Hilden, Germany) and treated with Turbo DNA-free DNase (AM 1907, Thermo Fisher Scientific Inc) following the manufacturer's protocol. The quantity and quality of the RNA samples were determined using the Agilent 2100 Bioanalyzer with RNA 6000 Nano Kit (5067-1511; Agilent Technologies, Santa Clara, CA). Total RNA (1  $\mu\text{g}$ ) was reverse transcribed with the High-Capacity cDNA Reverse Transcription Kit (Thermo Fisher Scientific Inc). Real-time quantitative polymerase chain reaction (PCR) was performed in duplicate for each sample using the StepOne Plus Real-Time PCR System (Thermo Fisher Scientific Inc) as previously described.<sup>53,65,66</sup> TaqMan gene expression assays were purchased from Thermo Fisher Scientific Inc: *RPLP0* (Hs99999902\_m1) (Mm99999223\_gH); *B2m* (Mm00437762\_m1); *Syk* (Mm01333032\_m1; Hs00895377\_m1); *Sh3bp2* (Mm00449397\_m1; Hs00610068\_m1); *Syk (L)* (Mm00441647\_m1); *Syk (S)* (Mm01333035\_m1); *Emr1* (Mm00802529\_m1); *Cd44* (Mm01277163\_m1); *Tnf* (Mm00443258\_m1); *Ccl2* (Mm00441242\_m1); *Sele* (Mm01310197\_m1); *Itgax* (Mm00498698\_m1); *Clec10a* (Mm00546124\_m1); *Tgfb1* (Mm03024053\_m1); *Timp1* (Mm00441818\_m1); *Col1a1* (Mm00801666\_g1); *Cyba* (Mm00514478\_m1); *Hmox1* (Mm00516005\_m1), *CD68* (Hs00154355\_m1), *Il6* (Mm00446190\_m1), *Il1b* (Mm00434228m1), *Trem1* (Mm01278455\_m1), and *Dap12* (Mm00449152\_m1). Gene expression was normalized to the  $\beta 2m$  ( $\beta 2$  microglobulin, mouse) or *RPLP0* (Ribosomal Phosphoprotein Large P0, mouse and human) housekeeping genes and calculated on the basis of the comparative cycle threshold Ct method ( $2^{-\Delta\Delta C_t}$ ). Gene expression was normalized to the *RPLP0*/36b4 housekeeping gene (human and mouse) and calculated on the basis of the comparative cycle threshold Ct method ( $2^{-\Delta\Delta C_t}$ ).

### Immunoblotting

Cells or frozen tissues were solubilized in lysis buffer (20 mmol/L Tris, pH 7.4, 150 mmol/L NaCl, 10 mmol/L EDTA, 150 mmol/L NaF, 2 mmol/L sodium orthovanadate, 10 mmol/L pyrophosphate, protease inhibitor cocktail, 1% Triton X-100, and okadaic acid) for 45 minutes at 4°C. Lysates were cleared (14,000 rpm, 15 minutes). Proteins were quantified (BCA Protein assay kit, 23225; Thermo Fisher Scientific Inc), separated by sodium dodecyl sulfate-

polyacrylamide gel electrophoresis, and immunoblotted as previously described.<sup>53</sup> The proteins were probed with Anti-SYK (#2712; Cell Signaling Technology), Anti-CD44 (AF6127; Bio-Techne), Anti-phospho SYK (Tyr<sup>525/526</sup>) (#2710; Cell Signaling Technology), Anti-p44/42 MAPK (#4695; Cell Signaling Technology), Anti-phospho-p44/42 MAPK (Thr<sup>202</sup>/Tyr<sup>204</sup>) (#9101; Cell Signaling Technology), and anti-HSP60 (K-19) (sc-1722; Santa Cruz Biotechnology, Dallas, TX) antibodies at 1  $\mu\text{g}/\text{mL}$  (Cell Signaling Technology) or at 1/1000 (Santa Cruz Biotechnology) as indicated.

### Statistical Analysis

Statistical significance between 2 human or mouse study groups was determined using the non-parametric Mann-Whitney test. Data from cell lines were analyzed using the Student *t* test. Spearman's correlation test was used for the correlative analysis. Results were considered significant for  $P < .05$ .

### References

1. Eslam M, Sanyal AJ, George J, International Consensus P. MAFLD: a consensus-driven proposed nomenclature for metabolic associated fatty liver disease. *Gastroenterology* 2020;158:1999–2014 e1.
2. Younossi ZM, Koenig AB, Abdelatif D, Fazel Y, Henry L, Wymer M. Global epidemiology of nonalcoholic fatty liver disease: meta-analytic assessment of prevalence, incidence, and outcomes. *Hepatology* 2016;64:73–84.
3. Swinburn BA, Sacks G, Hall KD, McPherson K, Finegood DT, Moodie ML, Gortmaker SL. The global obesity pandemic: shaped by global drivers and local environments. *Lancet* 2011;378:804–814.
4. Samuel VT, Shulman GI. Nonalcoholic fatty liver disease as a nexus of metabolic and hepatic diseases. *Cell Metab* 2018;27:22–41.
5. Raff EJ, Kakati D, Bloomer JR, Shoreibah M, Rasheed K, Singal AK. Diabetes mellitus predicts occurrence of cirrhosis and hepatocellular cancer in alcoholic liver and non-alcoholic fatty liver diseases. *J Clin Transl Hepatol* 2015;3:9–16.
6. Lallukka S, Yki-Jarvinen H. Non-alcoholic fatty liver disease and risk of type 2 diabetes. *Best Pract Res Clin Endocrinol Metab* 2016;30:385–395.
7. Targher G, Day CP, Bonora E. Risk of cardiovascular disease in patients with nonalcoholic fatty liver disease. *N Engl J Med* 2010;363:1341–1350.
8. Tran A, Gual P. Non-alcoholic steatohepatitis in morbidly obese patients. *Clin Res Hepatol Gastroenterol* 2013; 37:17–29.
9. Luci C, Bourinet M, Leclère PS, Anty R, Gual P. Chronic inflammation in non-alcoholic steatohepatitis: molecular mechanisms and therapeutic strategies. *Front Endocrinol* 2020;11:597648.
10. Cai J, Zhang XJ, Li H. The role of innate immune cells in nonalcoholic steatohepatitis. *Hepatology* 2019; 70:1026–1037.
11. Kazankov K, Jorgensen SMD, Thomsen KL, Moller HJ, Vilstrup H, George J, Schuppan D, Gronbaek H. The role



- of macrophages in nonalcoholic fatty liver disease and nonalcoholic steatohepatitis. *Nat Rev Gastroenterol Hepatol* 2019;16:145–159.
12. Lefere S, Tacke F. Macrophages in obesity and non-alcoholic fatty liver disease: crosstalk with metabolism. *JHEP Rep* 2019;1:30–43.
  13. Mocsai A, Ruland J, Tybulewicz VL. The SYK tyrosine kinase: a crucial player in diverse biological functions. *Nat Rev Immunol* 2010;10:387–402.
  14. Dennehy KM, Ferwerda G, Faro-Trindade I, Pyz E, Willment JA, Taylor PR, Kerrigan A, Tsoni SV, Gordon S, Meyer-Wentrup F, Adema GJ, Kullberg BJ, Schweighoffer E, Tybulewicz V, Mora-Montes HM, Gow NA, Williams DL, Netea MG, Brown GD. Syk kinase is required for collaborative cytokine production induced through Dectin-1 and Toll-like receptors. *Eur J Immunol* 2008;38:500–506.
  15. Miller YI, Choi SH, Wiesner P, Bae YS. The SYK side of TLR4: signalling mechanisms in response to LPS and minimally oxidized LDL. *Br J Pharmacol* 2012;167:990–999.
  16. Zewinger S, Reiser J, Jankowski V, Alansary D, Hahn E, Triem S, Klug M, Schunk SJ, Schmit D, Kramann R, Korbel C, Ampofo E, Laschke MW, Selejan SR, Paschen A, Herter T, Schuster S, Silbernagel G, Sester M, Sester U, Assmann G, Bals R, Kostner G, Jahnen-Dechent W, Menger MD, Rohrer L, Marz W, Bohm M, Jankowski J, Kopf M, Latz E, Niemeyer BA, Fliser D, Laufs U, Speer T. Apolipoprotein C3 induces inflammation and organ damage by alternative inflammasome activation. *Nat Immunol* 2020;21:30–41.
  17. Qu C, Zheng D, Li S, Liu Y, Lidofsky A, Holmes JA, Chen J, He L, Wei L, Liao Y, Yuan H, Jin Q, Lin Z, Hu Q, Jiang Y, Tu M, Chen X, Li W, Lin W, Fuchs BC, Chung RT, Hong J. Tyrosine kinase SYK is a potential therapeutic target for liver fibrosis. *Hepatology* 2018;68:1125–1139.
  18. Torres-Hernandez A, Wang W, Nikiforov Y, Tejada K, Torres L, Kalabin A, Wu Y, Haq MIU, Khan MY, Zhao Z, Su W, Camargo J, Hundeyin M, Diskin B, Adam S, Rossi JAK, Kurz E, Aykut B, Shadaloey SAA, Leinwand J, Miller G. Targeting SYK signaling in myeloid cells protects against liver fibrosis and hepatocarcinogenesis. *Oncogene* 2019;38:4512–4526.
  19. Afifiyan N, Tillman B, French BA, Masouminia M, Samadzadeh S, French SW. Over expression of proteins that alter the intracellular signaling pathways in the cytoplasm of the liver cells forming Mallory-Denk bodies. *Exp Mol Pathol* 2017;102:106–114.
  20. Pamuk ON, Can G, Ayzavaz S, Karaca T, Pamuk GE, Demirtas S, Tsokos GC. Spleen tyrosine kinase (Syk) inhibitor fostamatinib limits tissue damage and fibrosis in a bleomycin-induced scleroderma mouse model. *Clin Exp Rheumatol* 2015;33(Suppl 91):S15–S22.
  21. Ma FY, Blease K, Nikolic-Paterson DJ. A role for spleen tyrosine kinase in renal fibrosis in the mouse obstructed kidney. *Life Sci* 2016;146:192–200.
  22. Weinblatt ME, Kavanaugh A, Genovese MC, Musser TK, Grossbard EB, Magilavy DB. An oral spleen tyrosine kinase (Syk) inhibitor for rheumatoid arthritis. *N Engl J Med* 2010;363:1303–1312.
  23. Sun H, Feng J, Tang L. Function of TREM1 and TREM2 in liver-related diseases. *Cells* 2020;9(12).
  24. Tornai D, Furi I, Shen ZT, Sigalov AB, Coban S, Szabo G. Inhibition of triggering receptor expressed on myeloid cells 1 ameliorates inflammation and macrophage and neutrophil activation in alcoholic liver disease in mice. *Hepatol Commun* 2019;3:99–115.
  25. Nguyen-Lefebvre AT, Ajith A, Portik-Dobos V, Horuzsko DD, Arbab AS, Dzutsev A, Sadek R, Trinchieri G, Horuzsko A. The innate immune receptor TREM-1 promotes liver injury and fibrosis. *J Clin Invest* 2018;128:4870–4883.
  26. Wang L, Aschenbrenner D, Zeng Z, Cao X, Mayr D, Mehta M, Capitani M, Warner N, Pan J, Wang L, Li Q, Zuo T, Cohen-Kedar S, Lu J, Ardy RC, Mulder DJ, Dissanayake D, Peng K, Huang Z, Li X, Wang Y, Wang X, Li S, Bullers S, Gammage AN, Warnatz K, Schiefer AI, Krivan G, Goda V, Kahr WHA, Lemaire M, Genomics England Research C, Lu CY, Siddiqui I, Surette MG, Kotlarz D, Engelhardt KR, Griffin HR, Rottapel R, Decaluwe H, Laxer RM, Proietti M, Hambleton S, Elcombe S, Guo CH, Grimbacher B, Dotan I, Ng SC, Freeman SA, Snapper SB, Klein C, Boztug K, Huang Y, Li D, Uhlig HH, Muise AM. Gain-of-function variants in SYK cause immune dysregulation and systemic inflammation in humans and mice. *Nat Genet* 2021;53:500–510.
  27. Deckert M, Tartare-Deckert S, Hernandez J, Rottapel R, Altman A. Adaptor function for the Syk kinases-interacting protein 3BP2 in IL-2 gene activation. *Immunity* 1998;9:595–605.
  28. Deckert M. [The adaptor protein 3BP2 in leukocyte signaling]. *Med Sci (Paris)* 2006;22:1081–1086.
  29. Foucault I, Le Bras S, Charvet C, Moon C, Altman A, Deckert M. The adaptor protein 3BP2 associates with VAV guanine nucleotide exchange factors to regulate NFAT activation by the B-cell antigen receptor. *Blood* 2005;105:1106–1113.
  30. GuezGuez A, Prod'homme V, Mouska X, Baudot A, Blin-Wakkach C, Rottapel R, Deckert M. 3BP2 adapter protein is required for receptor activator of NFkappaB ligand (RANKL)-induced osteoclast differentiation of RAW264.7 cells. *J Biol Chem* 2010;285:20952–20963.
  31. Prod'Homme V, Boyer L, Dubois N, Mallavialle A, Munro P, Mouska X, Coste I, Rottapel R, Tartare-Deckert S, Deckert M. Cherubism allele heterozygosity amplifies microbe-induced inflammatory responses in murine macrophages. *J Clin Invest* 2015;125:1396–1400.
  32. Ueki Y, Tiziani V, Santanna C, Fukai N, Maulik C, Garfinkle J, Ninomiya C, doAmaral C, Peters H, Habal M, Rhee-Morris L, Doss JB, Kreiborg S, Olsen BR, Reichenberger E. Mutations in the gene encoding c-Abl-binding protein SH3BP2 cause cherubism. *Nat Genet* 2001;28:125–126.
  33. Ueki Y, Lin CY, Senoo M, Ebihara T, Agata N, Onji M, Saheki Y, Kawai T, Mukherjee PM, Reichenberger E, Olsen BR. Increased myeloid cell responses to M-CSF

- and RANKL cause bone loss and inflammation in SH3BP2 "cherubism" mice. *Cell* 2007;128:71–83.
34. Deckert M, Prod'Homme V. [SH3BP2 heterozygous mutation amplifies macrophage inflammatory responses to infection in a mouse model of cherubism]. *Med Sci (Paris)* 2015;31:589–591.
  35. Reichenberger EJ, Levine MA, Olsen BR, Papadaki ME, Lietman SA. The role of SH3BP2 in the pathophysiology of cherubism. *Orphanet J Rare Dis* 2012;7(Suppl 1):S5.
  36. Yoshitaka T, Mukai T, Kittaka M, Alford LM, Masrani S, Ishida S, Yamaguchi K, Yamada M, Mizuno N, Olsen BR, Reichenberger EJ, Ueki Y. Enhanced TLR-MYD88 signaling stimulates autoinflammation in SH3BP2 cherubism mice and defines the etiology of cherubism. *Cell Rep* 2014;8:1752–1766.
  37. Yoshimoto T, Hayashi T, Kondo T, Kittaka M, Reichenberger EJ, Ueki Y. Second-generation SYK inhibitor entospletinib ameliorates fully established inflammation and bone destruction in the cherubism mouse model. *J Bone Miner Res* 2018;33:1513–1519.
  38. Bertola A, Park O, Gao B. Chronic plus binge ethanol feeding synergistically induces neutrophil infiltration and liver injury in mice: a critical role for E-selectin. *Hepatology* 2013;58:1814–1823.
  39. Turner M, Mee PJ, Costello PS, Williams O, Price AA, Duddy LP, Furlong MT, Geahlen RL, Tybulewicz VL. Perinatal lethality and blocked B-cell development in mice lacking the tyrosine kinase Syk. *Nature* 1995;378:298–302.
  40. Cheng AM, Rowley B, Pao W, Hayday A, Bolen JB, Pawson T. Syk tyrosine kinase required for mouse viability and B-cell development. *Nature* 1995;378:303–306.
  41. Kurniawan DW, Jajoriya AK, Dhawan G, Mishra D, Argemi J, Bataller R, Storm G, Mishra DP, Prakash J, Bansal R. Therapeutic inhibition of spleen tyrosine kinase in inflammatory macrophages using PLGA nanoparticles for the treatment of non-alcoholic steatohepatitis. *J Control Release* 2018;288:227–238.
  42. Levaot N, Voytyuk O, Dimitriou I, Sircoulomb F, Chandrakumar A, Deckert M, Krzyzanowski PM, Scotter A, Gu S, Janmohamed S, Cong F, Simoncic PD, Ueki Y, La Rose J, Rottapel R. Loss of Tankyrase-mediated destruction of 3BP2 is the underlying pathogenic mechanism of cherubism. *Cell* 2011;147:1324–1339.
  43. de Jesus AA, Canna SW, Liu Y, Goldbach-Mansky R. Molecular mechanisms in genetically defined auto-inflammatory diseases: disorders of amplified danger signaling. *Annu Rev Immunol* 2015;33:823–874.
  44. Levaot N, Simoncic PD, Dimitriou ID, Scotter A, La Rose J, Ng AH, Willett TL, Wang CJ, Janmohamed S, Grynopas M, Reichenberger E, Rottapel R. 3BP2-deficient mice are osteoporotic with impaired osteoblast and osteoclast functions. *J Clin Invest* 2011;121:3244–3257.
  45. Zhao GN, Zhang P, Gong J, Zhang XJ, Wang PX, Yin M, Jiang Z, Shen LJ, Ji YX, Tong J, Wang Y, Wei QF, Wang Y, Zhu XY, Zhang X, Fang J, Xie Q, She ZG, Wang Z, Huang Z, Li H. Tmbim1 is a multivesicular body regulator that protects against non-alcoholic fatty liver disease in mice and monkeys by targeting the lysosomal degradation of Tlr4. *Nat Med* 2017;23:742–752.
  46. Li L, Chen L, Hu L, Liu Y, Sun HY, Tang J, Hou YJ, Chang YX, Tu QQ, Feng GS, Shen F, Wu MC, Wang HY. Nuclear factor high-mobility group box1 mediating the activation of Toll-like receptor 4 signaling in hepatocytes in the early stage of nonalcoholic fatty liver disease in mice. *Hepatology* 2011;54:1620–1630.
  47. Karlmark KR, Weiskirchen R, Zimmermann HW, Gassler N, Ginhoux F, Weber C, Merad M, Luedde T, Trautwein C, Tacke F. Hepatic recruitment of the inflammatory Gr1+ monocyte subset upon liver injury promotes hepatic fibrosis. *Hepatology* 2009;50:261–274.
  48. Seki E, de Minicis S, Inokuchi S, Taura K, Miyai K, van Rooijen N, Schwabe RF, Brenner DA. CCR2 promotes hepatic fibrosis in mice. *Hepatology* 2009;50:185–197.
  49. Baeck C, Wehr A, Karlmark KR, Heymann F, Vucur M, Gassler N, Huss S, Klussmann S, Eulberg D, Luedde T, Trautwein C, Tacke F. Pharmacological inhibition of the chemokine CCL2 (MCP-1) diminishes liver macrophage infiltration and steatohepatitis in chronic hepatic injury. *Gut* 2012;61:416–426.
  50. Parker R, Weston CJ, Miao Z, Corbett C, Armstrong MJ, Ertl L, Ebsworth K, Walters MJ, Baumart T, Newland D, McMahon J, Zhang P, Singh R, Campbell J, Newsome PN, Charo I, Schall TJ, Adams DH. CC chemokine receptor 2 promotes recruitment of myeloid cells associated with insulin resistance in nonalcoholic fatty liver disease. *Am J Physiol Gastrointest Liver Physiol* 2018;314:G483–G493.
  51. Bertola A, Bonnafous S, Anty R, Patouraux S, Saint-Paul MC, Iannelli A, Gugenheim J, Barr J, Mato JM, Le Marchand-Brustel Y, Tran A, Gual P. Hepatic expression patterns of inflammatory and immune response genes associated with obesity and NASH in morbidly obese patients. *PLoS One* 2010;5:e13577.
  52. Krenkel O, Puengel T, Govaere O, Abdallah AT, Mossanen JC, Kohlhepp M, Liepelt A, Lefebvre E, Luedde T, Hellerbrand C, Weiskirchen R, Longerich T, Costa IG, Anstee QM, Trautwein C, Tacke F. Therapeutic inhibition of inflammatory monocyte recruitment reduces steatohepatitis and liver fibrosis. *Hepatology* 2018;67:1270–1283.
  53. Patouraux S, Rousseau D, Bonnafous S, Lebeaupin C, Luci C, Canivet CM, Schneck AS, Bertola A, Saint-Paul MC, Iannelli A, Gugenheim J, Anty R, Tran A, Bailly-Maitre B, Gual P. CD44 is a key player in non-alcoholic steatohepatitis. *J Hepatol* 2017;67:328–338.
  54. Ibrahim SH, Hirsova P, Gores GJ. Non-alcoholic steatohepatitis pathogenesis: sublethal hepatocyte injury as a driver of liver inflammation. *Gut* 2018;67:963–972.
  55. Gautheron J, Gores GJ, Rodrigues CMP. Lytic cell death in metabolic liver disease. *J Hepatol* 2020;73:394–408.
  56. Liss KH, Finck BN. PPARs and nonalcoholic fatty liver disease. *Biochimie* 2017;136:65–74.
  57. Ip E, Farrell GC, Robertson G, Hall P, Kirsch R, Leclercq I. Central role of PPARalpha-dependent hepatic

- lipid turnover in dietary steatohepatitis in mice. *Hepatology* 2003;38:123–132.
58. Ip E, Farrell G, Hall P, Robertson G, Leclercq I. Administration of the potent PPAR $\alpha$  agonist, Wy-14,643, reverses nutritional fibrosis and steatohepatitis in mice. *Hepatology* 2004;39:1286–1296.
  59. Bukong TN, Iracheta-Vellve A, Gyongyosi B, Ambade A, Catalano D, Kodys K, Szabo G. Therapeutic benefits of spleen tyrosine kinase inhibitor administration on binge drinking-induced alcoholic liver injury, steatosis, and inflammation in mice. *Alcohol Clin Exp Res* 2016;40:1524–1530.
  60. Chen G, Dimitriou ID, La Rose J, Ilangumaran S, Yeh WC, Doody G, Turner M, Gommerman J, Rottapel R. The 3BP2 adapter protein is required for optimal B-cell activation and thymus-independent type 2 humoral response. *Mol Cell Biol* 2007;27:3109–3122.
  61. Bekri S, Gual P, Anty R, Luciani N, Dahman M, Ramesh B, Iannelli A, Staccini-Myx A, Casanova D, Ben Amor I, Saint-Paul MC, Huet PM, Sadoul JL, Gugenheim J, Srai SK, Tran A, Le Marchand-Brustel Y. Increased adipose tissue expression of hepcidin in severe obesity is independent from diabetes and NASH. *Gastroenterology* 2006;131:788–796.
  62. Anty R, Bekri S, Luciani N, Saint-Paul MC, Dahman M, Iannelli A, Ben Amor I, Staccini-Myx A, Huet PM, Gugenheim J, Sadoul JL, Le Marchand-Brustel Y, Tran A, Gual P. The inflammatory C-reactive protein is increased in both liver and adipose tissue in severely obese patients independently from metabolic syndrome, type 2 diabetes, and NASH. *Am J Gastroenterol* 2006;101:1824–1833.
  63. Wallace TM, Levy JC, Matthews DR. Use and abuse of HOMA modeling. *Diabetes Care* 2004;27:1487–1495.
  64. Kleiner DE, Brunt EM, Van Natta M, Behling C, Contos MJ, Cummings OW, Ferrell LD, Liu YC, Torbenson MS, Unalp-Arida A, Yeh M, McCullough AJ, Sanyal AJ. Design and validation of a histological scoring system for nonalcoholic fatty liver disease. *Hepatology* 2005;41:1313–1321.
  65. Sans A, Bonnafous S, Rousseau D, Patouraux S, Canivet CM, Leclere PS, Tran-Van-Nhieu J, Luci C, Bailly-Maitre B, Xu X, Lee AH, Minehira K, Anty R, Tran A, Iannelli A, Gual P. The differential expression of cide family members is associated with nafld progression from steatosis to steatohepatitis. *Sci Rep* 2019;9:7501.
  66. Canivet CM, Bonnafous S, Rousseau D, Leclere PS, Lacas-Gervais S, Patouraux S, Sans A, Luci C, Bailly-Maitre B, Iannelli A, Tran A, Anty R, Gual P. Hepatic FNDC5 is a potential local protective factor against non-alcoholic fatty liver. *Biochim Biophys Acta Mol Basis Dis* 2020;1866:165705.

Received March 6, 2021. Accepted August 10, 2021.

#### Correspondence

Address correspondence to: Philippe Gual, PhD, Inserm UMR1065/C3M, Bâtiment Universitaire ARCHIMED, Team "Chronic liver diseases associated with obesity and alcohol", 151 route Saint Antoine de Ginestière, BP 2 3194, 06204 Nice, France. e-mail: philippe.gual@inserm.fr; fax: +33 4 89 06 42 60. Marcel Deckert, PhD, Inserm UMR1065/C3M, Bâtiment Universitaire ARCHIMED, Team "Microenvironment, signaling and cancer", 151 route Saint Antoine de Ginestière, BP 2 3194, 06204 Nice, France. e-mail: marcel.deckert@inserm.fr.

#### Acknowledgments

The authors thank the INSERM U1065 animal facility staff and Dr V. Corcelle, the INSERM U1065 flow cytometry platform, Dr Jeanne Tran-Van-Nhieu (HU Henri Mondor, Department of Pathology, AP-HP - Université Paris Est Créteil, Créteil, France) for providing the liver tissues from lean subjects, and Professor Robert Rottapel (Princess Margaret Cancer Center, University of Toronto, Toronto, Canada) for providing the Sh3bp2 KO mice.

#### CRedit Authorship Contributions

Carmelo Luci, PhD (Formal analysis: Equal; Investigation: Equal; Methodology: Equal; Project administration: Equal; Writing – review & editing: Equal)

Elodie Vieira, PhD (Formal analysis: Equal; Investigation: Equal; Methodology: Equal; Writing – review & editing: Supporting)

Manon Bourinet (Formal analysis: Supporting; Investigation: Supporting; Methodology: Supporting; Writing – review & editing: Supporting)

Déborah Rousseau, PhD (Formal analysis: Supporting; Investigation: Supporting; Methodology: Supporting; Writing – review & editing: Supporting)

Stéphanie Bonnafous (Formal analysis: Supporting; Investigation: Supporting; Methodology: Supporting; Writing – review & editing: Supporting)

Stéphanie Patouraux, PhD, MD (Formal analysis: Supporting; Investigation: Supporting; Writing – review & editing: Supporting)

Lauren Lefevre (Formal analysis: Supporting; Investigation: Supporting; Writing – review & editing: Supporting)

Frederic Larbret, PhD (Formal analysis: Supporting; Investigation: Supporting; Writing – review & editing: Supporting)

Virginie Prod'homme, PhD (Formal analysis: Supporting; Investigation: Supporting; Writing – review & editing: Supporting)

Antonio Iannelli, PhD, MD (Writing – review & editing: Supporting; Human liver biopsies: Lead)

Albert Tran, PhD, MD (Writing – review & editing: Supporting; Human liver biopsies: Lead)

Rodolphe Anty, PhD, MD (Writing – review & editing: Supporting; Human liver biopsies: Lead)

Béatrice Bailly-Maitre, PhD (Funding acquisition: Supporting; Writing – review & editing: Supporting)

Marcel Deckert, PhD (Conceptualization: Lead; Formal analysis: Lead; Funding acquisition: Lead; Supervision: Equal; Validation: Equal; Writing – review & editing: Lead)

Philippe Gual, PhD (Conceptualization: Lead; Formal analysis: Lead; Funding acquisition: Lead; Investigation: Lead; Project administration: Lead; Supervision: Lead; Writing – original draft: Lead; Writing – review & editing: Lead)

#### Conflicts of interest

The authors disclose no conflicts.

#### Funding

Supported by grants from INSERM (France), charities (Association Française pour l'Etude du Foie (AFEF) to PG, Société Francophone du Diabète (SFD) to PG, SFD/Roche Pharma to PG, and SFD and LifeScan to BBM. This work was also funded by the French Government (National Research Agency, ANR): #ANR-18-CE14-0019-01, #ANR-18-CE14-0019-02, #ANR-18-CE14-0022-01, #ANR-19-CE14-0044-01, and through the "Investments for the Future" LABEX SIGNALIFE (#ANR-11-LABX-0028-01) and the UCA<sup>JEDI</sup> Investments in the Future project (#ANR-15-IDEX-01). EV was supported by a PhD grant from the Fondation pour la Recherche Médicale and LL and MB by the ANR (#ANR-18-CE14-0019-01 and #ANR-18-CE14-0019-02, respectively). MB is currently supported by a doctoral fellowship from French Ministry of Research.